E&G Quaternary Sci. J., 73, 41–67, 2024
https://doi.org/10.5194/egqsj-73-41-2024

Open Access E&G Quaternary Science Journal

Research article

Loess formation and chronology at the Palaeolithic key site Rheindahlen, Lower Rhine Embayment, Germany

Martin Kehl[1,2], Katharina Seeger[2], Stephan Pötter[1,3], Philipp Schulte[3], Nicole Klasen[2], Mirijam Zickel[2], Andreas Pastoors[4], and Erich Claßen[5]

[1]Department of Geography, University of Koblenz, Universitätsstraße 1, 56070 Koblenz, Germany
[2]Institute of Geography, University of Cologne, Albertus-Magnus-Platz, 50923 Cologne, Germany
[3]Chair of Physical Geography and Geoecology, RWTH Aachen University, Templergraben 55, 52056 Aachen, Germany
[4]Institut für Ur- und Frühgeschichte, Friedrich-Alexander-Universität Erlangen-Nürnberg, Kochstr. 4–18, 91054 Erlangen, Germany
[5]LVR-Amt für Bodendenkmalpflege im Rheinland, Endenicher Str. 133, 53115 Bonn, Germany

Correspondence: Martin Kehl (kehlm@uni-koblenz.de)

Relevant dates: Received: 1 February 2023 – Revised: 8 November 2023 – Accepted: 16 November 2023 – Published: 26 January 2024

How to cite: Kehl, M., Seeger, K., Pötter, S., Schulte, P., Klasen, N., Zickel, M., Pastoors, A., and Claßen, E.: Loess formation and chronology at the Palaeolithic key site Rheindahlen, Lower Rhine Embayment, Germany, E&G Quaternary Sci. J., 73, 41–67, https://doi.org/10.5194/egqsj-73-41-2024, 2024.

Abstract: The loess–palaeosol sequence and intercalated Palaeolithic find layers at the former brickyard of Rheindahlen are matters of ongoing scientific dispute. The age of different palaeosols and loess layers, hence their correlation with the global climate cycles, and the timing of repeated Neanderthal occupations have been hotly debated. These disagreements should be solved because the exceptional sedimentary and Palaeolithic sequences at Rheindahlen provide a unique opportunity to study diachronic changes in Neanderthal behaviour within the context of past climate change. We thus revisited one of the key loess sections of the Rheindahlen site to improve our understanding of loess formation processes and provide a more reliable chronostratigraphic framework for the sequence. High-resolution grain size analyses and micromorphology show that the Erkelenz Soil and the Rheindahlen Soil are characterized by more strongly developed Bt horizons than the modern soil. While these soils represent interglacial phases, the lowermost palaeosol likely formed during an interstadial and has been overprinted by weak clay illuviation during the formation of the Rheindahlen Soil. Sedimentary features of prolonged frost characterize loess and palaeosols below the modern soil and give indirect evidence for a Holocene age of the uppermost part of the sequence. Our luminescence dating approach corroborates this correlation and adds several Last Glacial deposition ages for the upper metres of the sequence. Previous correlation of this part of the sedimentary sequence with the penultimate glacial is thus rejected, whereas placing the Middle Palaeolithic inventories A3, B1, and B2 into the Last Glacial is confirmed. Luminescence measurements for the parental loess of the Erkelenz Soil and for loess layers below did not provide reliable ages probably related to signal saturation. The age of this part of the sequence thus remains open, hence the timing of human occupation testified by Palaeolithic inventories B3, B4/5, C1, and D1. The new findings provide an improved base for stratigraphic correlation of the Rheindahlen loess sequence and for investigating diachronic change in Neanderthal behaviour against the background of past climate change.

Published by Copernicus Publications on behalf of the Deutsche Quartärvereinigung (DEUQUA) e.V.

Kurzfassung:

Die Lössstratigraphie in der ehemaligen Ziegelei Rheindahlen sowie ihre stratifizierten paläolithischen Fundhorizonte sind wissenschaftlich umstritten. Das Alter der Paläoböden und Lössschichten und damit ihre Korrelation mit globalen Klimazyklen als auch der Zeitpunkt der wiederholten Besiedlung durch den Neanderthaler werden kontrovers diskutiert. Diese Unstimmigkeiten sollten ausgeräumt werden, denn die sedimentären und archäologischen Abfolgen in Rheindahlen bieten eine einzigartige Gelegenheit, diachrone Veränderungen im Verhalten der Neanderthaler im Kontext vergangener Klimaveränderungen zu untersuchen. Wir haben daher eines der wichtigsten Lössprofile von Rheindahlen neu untersucht, um unser Verständnis der Lössbildung zu verbessern und einen zuverlässigen chronostratigraphischen Rahmen für die Abfolge aufzustellen. Hochauflösende Korngrößenanalysen und Mikromorphologie zeigen, dass der Erkelenz-Boden und der Rheindahlen-Boden durch stärker ausgeprägte Bt-Horizonte gekennzeichnet sind als der rezente Boden. Während diese Böden interglaziale Phasen repräsentieren, ist der unterste Paläoboden wahrscheinlich während eines Interstadials entstanden und wurde während der Bildung des Rheindahlen-Bodens von einer schwachen Toninfiltration überprägt. Sedimentäre Merkmale von anhaltendem Frost charakterisieren Löss und Paläoböden unterhalb des rezenten Bodens und ihr Fehlen im oberen Teil liefert indirekte Hinweise auf sein holozänes Alter. Unsere Lumineszenzdatierungen bestätigen diese Korrelation und liefern mehrere letztglaziale Ablagerungsalter für die oberen Meter der Sedimentabfolge, so dass eine Korrelation dieses Teils mit dem vorletzten Glazial abgelehnt wird. Die mittelpaläolithischen Inventare A3, B1, und B2 sind somit in das letzte Glazial zu stellen. Die Lumineszenzmessungen der Lössschichten des Erkelenz-Bodens und unterhalb folgender Schichten lieferten keine zuverlässigen Alter, was wahrscheinlich auf Signalsättigung zurückzuführen ist. Die Alter dieses Teils der Abfolge und der durch die paläolithischen Inventare B3, B4/5, C1 und D1 dokumentierten Besiedlungen bleiben daher offen. Die neuen Befunde bieten eine verbesserte Grundlage für die stratigraphische Einordnung der Lössabfolge von Rheindahlen und für die Interpretation möglicher diachroner Veränderungen im Verhalten des Neanderthalers vor dem Hintergrund vergangener Klimaveränderungen.

1 Introduction

Loess–palaeosol sequences (LPSs) are excellent geological archives for the study of palaeoenvironmental dynamics which can often be regarded as continuous terrestrial records of past climate and landscape evolution and show close correlation with ice-core records and other high-resolution archives (e.g. Antoine et al., 2009; Haesaerts et al., 2016; Moine et al., 2017; Marković et al., 2018; Fischer et al., 2021). However, loess sections in Central and Western Europe frequently show stratigraphic discontinuities and inclusion of reworked loess facies (e.g. Sabelberg et al., 1976; Meijs et al., 2013; Lehmkuhl et al., 2016; Antoine et al., 2021). Such stratigraphic gaps may represent short phases of the past like in the exceptionally well-preserved Last Pleniglacial records of Remagen Schwalbenberg (Schirmer, 2016; Fischer et al., 2021) and Nussloch (Bibus et al., 2007; Antoine et al., 2009) or cover whole glacial periods as postulated for the LPS at Rheindahlen (Schirmer, 2002) or supported by chronometric evidence at Köndringen (Schwahn et al., 2023). In the Lower Rhine Embayment, LPSs have been exposed in several brickyards and large-scale lignite open cast mines, partly in very broad lateral extent (e.g. Henze, 1998; Kels, 2007; Fischer et al., 2012), providing ample opportunities for detailed loess investigations. The current notion is that the regional loess stratigraphy encompasses several Middle to Upper Pleistocene pedocomplexes and loess layers probably covering four interglacial–glacial climate cycles (Schirmer, 2016). The loess record of the Last Glacial is characterized by several disconformities, and it appears that the Early and Middle Pleniglacial parts are rarely preserved (Lehmkuhl et al., 2016).

The LPS at Rheindahlen has been studied since the 1960s (Paas, 1962, 1992; Brunnacker, 1966; Bosinksi and Brunnacker, 1973; Thieme et al., 1981; Schirmer and Feldmann, 1992; Schirmer, 1992, 1999, 2002). Authors mostly agree in stratigraphic site description, but they identify different numbers of Bt and Bw horizons partly related to different sections studied in the course of loess excavation over several decades. In the Western and Central European loess stratigraphy, Bt horizons are interpreted as markers of interglacial stages because similar subsoil horizons are characteristic for Luvisols mostly formed under forest vegetation on loess during the Holocene (Zöller and Semmel, 2001). Instead, Bw horizons are often correlated with interstadial soil formation during glacial stages. Based on counting Bt horizons from the top and consideration of erosional discontinuities, authors come to quite different conclusions about the timing of loess and palaeosol formation at Rheindahlen. The different views are illustrated by the three chronostratigraphic schemes listed in Table 1 which extend down to MIS 8 (Paas, 1992; Schirmer, 2002) or MIS 12 (Klostermann and Thissen,

Table 1. General schemes of the loess–palaeosol sequence and stratigraphic position of archaeological layers at Rheindahlen. Three chronostratigraphic models as proposed by different authors and previous thermoluminescence age estimates for selected loess units of the LPS at Rheindahlen are listed.

Unit[1]	Archaeological layer	Paas (1992)		Klostermann and Thissen (1995)		Schirmer (2002)		Thermoluminescence ages	
		Stratigraphic unit	MIS[4]	Stratigraphic unit	MIS[5]	Stratigraphic unit	MIS[6]	Frechen et al. (1992)	Zöller et al. (1988), Zöller (1989)
Topmost soil (Bt)	A1 LP[2]	Bt #1: Holocene	*1*	Bt #1: Holocene	1	Bt #1: Holocene Bt #2: Eemian	*1* 5	–	–
Loess loam (*Braunlöss*)	A2 MP[3] A3 MP	Loess loam, Weichselian	*2–4*	Loess loam; Weichselian	*2–4*	Wetterau Loess, Gilgau Loess	6	103 ka 99 ka	ca. 120 ka[7] 77 ka
White Band (*helles Band*)	B1 MP, B2 MP		*(5)*					> 163 ka	137 ka
Erkelenz Soil (Bt)		Bt #2: Eemian	*5e*	Bt #2: Eemian	*5(e)*	Bt #3: Erkelenz Soil	7a	> 142 ka	–
Loess loam (*Fleckenlehm/ Siltschmitzenlehm*)	B3 MP B4/5 MP	Loess loam and tundra gley, Upper Saalian ("Warthe")	*6*	Loess loam, Saalian ("Warthe, Drenthe")	6–8	Upper Limburg Loess, Erkelenz Marker, Middle Limburg Loess, Rheindahlen Humus Zone		(> 176–194 ka)	167 ka
Rheindahlen Soil (Bt)		Bt #3: Interglacial	*7*	Bt #3: Holsteinian	9	Bt #4: Rheindahlen Soil	7c	–	–
Loess loam (*Staublehm*)	C1 MP?	Loess loam, Lower Saalian ("Drenthe")	*8*	Loess loam, Elsterian complex	10	Lower Limburg Loess		(> 172–194 ka)	239 ka
Palaeosol (Bt/Bw)		Bw: Interstadial, Lower Saalian	*8*	Bt #4: Römerhof Interglacial	11	BtBw: Wickrath Soil	7e	–	–
Loess loam (*Staublehm*)	D1 MP?	Loess loam, Lower Saalian ("Drenthe")	*8*	Loess loam, Elsterian complex	12–13	Mülgau Loess	8	–	–
Sand and gravel		Younger upper terrace of the Rhine River							

[1] The general scheme is presented here; less strongly developed palaeosols are not shown. [2] Late Palaeolithic (LP) finds of layer A1 were found in the subrecent channel fill K1. [3] Middle Palaeolithic (MP) finds of layer A2 were detected in the Late Glacial channel fill K2. [4] Tentative correlation with marine isotope stages (MISs) according to Lisiecki and Raymo (2005); numbers in italics were supplemented for comparison by the authors based on Menning (2018). [5] Correlation with MIS according to Klostermann and Thissen (1995, Table 1: 52). [6] Schirmer (2002: 16) gives the correlation with the peaks of MIS 7.1, 7.3, and 7.5, not with the periods MIS 7a, 7c, and 7e. For simplicity, we adopted the latter correlation throughout this paper. [7] Zöller (1989).

https://doi.org/10.5194/egqsj-73-41-2024

1995) with significant differences in age assignments of loess loam or palaeosol layers. In the 1980–1990s, the sequence was dated twice by thermoluminescence and optically stimulated luminescence dating techniques (Zöller et al., 1988; Zöller, 1989; Frechen et al., 1992), but still no final conclusion about the chronology has been made.

The site Rheindahlen is famous for its Palaeolithic findings because it is the oldest site with stratified artefacts in North Rhine Westphalia and type locality for the Rheindahlien technocomplex (Bosinski, 1966, 2008). Due to the uncertainty in loess chronostratigraphy the age of the embedded find layers is debated: the upper layers (B2, B1, A3, A2, and A1) have been interpreted either as Eemian and younger (Thieme et al., 1981; Klostermann and Thissen, 1995; Thissen, 2006) (hereafter designated as the age model of Klostermann) or as pre-Eemian (Schirmer and Feldmann, 1992; Schirmer, 2002; E.-M. Ikinger, 2002) (hereafter designated as the age model of Schirmer). The timing of the lower find layers (B3, B4/5, and C1) is even less clear.

The dispute on the stratigraphy of the LPS and the timing of Palaeolithic occupation is not yet solved. Since the last excavations at Rheindahlen from 1995 to 2001 (Thissen, 2006), analytical methods have improved and a re-evaluation of the sequence may help us to solve the chronological issues. Such re-evaluation should involve a thorough understanding of loess formation deciphering syngenetic and post-depositional processes of dust accumulation, reworking, and pedogenesis. Besides detailed field descriptions, high-resolution sampling for granulometric and spectrophotometric analyses provides important information to decipher changes in loess deposition modes and post-depositional alteration. The micromorphological scale of investigation provides further insights into sediment composition and structure, thereby elucidating types of reworking and soil-forming processes. Ideally, the temporal sequence of processes can be reconstructed, allowing us to identify both diachronic change in pedogenesis and polygenetic overprint such as the illuviation of clay in loess layers. In this regard, micromorphological features formed by frost (e.g. under periglacial climate) help us to differentiate Holocene and Pleistocene processes. Micromorphology thus helps us to set up litho- and pedostratigraphies of the LPS at a certain site, providing the context for relative and absolute dating of sediment accumulation crucial to constrain missing episodes of the loess record.

A variety of studies have used pedostratigraphy, geochemical proxies, or fossil content and aligned these to oxygen isotope records for age correlation (e.g. Moine et al., 2008; Antoine et al., 2009; Buggle et al., 2009; Haesaerts et al., 2009; Schirmer, 2016; Vinnepand et al., 2022). Since the development of optically stimulated luminescence dating of sediments (Aitken, 1998), the numerical dating of LPSs (e.g. Roberts, 2008; Timar-Gabor et al., 2011; Lomax et al., 2014; Tecsa et al., 2020) has improved the chronological information about sediment deposition which is essential to correlate between records. However, for research questions targeting high-resolution palaeoclimatic information and occupational history, multi-method dating approaches in combination with various climate proxies (e.g. Rousseau et al., 2002; Moine et al., 2017; Újvári et al., 2017; Prud'homme et al., 2019) are necessary because dating uncertainties of several thousand years cannot provide age information in sufficient resolution (Blaauw et al., 2010). Therewith, the measurement uncertainty of the individual numerical results that are used for the development of age–depth models has become more and more important (Perić et al., 2019; Scheidt et al., 2021). In the Lower Rhine Embayment, luminescence dating led to new information about the chronology of the deposits and the palaeoenvironmental changes in the region (Klasen et al., 2015; Zens et al., 2018; Fischer et al., 2019).

By combining granulometric, spectrophotometric, micromorphological and luminescence dating techniques, we aim to re-investigate the profile studied by Schirmer (2002). In particular, our aim is to better reconstruct climate imprints and depositional processes by providing high-resolution granulometric data and microscale observations. In addition, we test different luminescence protocols with a multi-method optically stimulated luminescence dating approach using quartz and polymineral fine-grain sediments aiming to improve age control for loess layers and palaeosols and the related Palaeolithic find layers.

2 The site Rheindahlen

The study site is located at the southern edge of the town of Rheindahlen, where the two open-cast mines Dreesen and Dahmen have exposed 6–9 m thick loess deposits resting on top of fluvial sands and gravel of the upper terrace of the Rhine River. The exceptional thickness of the loess cover at this location is probably related to tectonic subsidence of the Venlo block south of the Rheindahlen fault, thereby promoting accumulation and preservation of dust (Paas, 1992; Klostermann and Thissen, 1995). Rheindahlen currently receives a mean annual precipitation of $\sim$ 800 mm and has a mean annual air temperature of $\sim$ 10.5 °C. Several profiles and walls of the brickyards have been studied and sketched during the second half of the 20th century as described in detail by Schirmer (2002). The sequence is locally accessible in the ca. 200 m long western wall of the former brickyard Dreesen, which is today covered by vegetation.

2.1 The Rheindahlen LPS and previous chronostratigraphic estimates

Loess at Rheindahlen is up to ca. 7 m thick and generally leached in carbonates, although the uppermost layer correlated with the Weichselian may locally still contain some carbonate (Thieme et al., 1981). The loess loam is divided by several palaeosols characterized by Bt or Bw horizons which represent remnants of former Luvisols or Cambisols, respectively. The palaeosol horizons are numbered from top

to bottom by the different authors, and two strongly developed ones with Bt horizons are denominated as Erkelenz Soil and Rheindahlen Soil (Table 1; Fig. 2).

The uppermost metre of the sequence consists of a former plough layer and a Bt horizon ascribed to the modern soil (Paas, 1962, 1992; Brunnacker, 1966; Thieme et al., 1981; Klostermann and Thissen, 1995). A gravel band observed in the lower part of this Bt horizon (Paas, 1992) indicates reworking by slope processes. Sandy intercalations (Paas, 1992; Schirmer, 2002) probably related to changes in the wind regime are reported, too, which is likely, since Rheindahlen is located near the southern boundary of periglacial sand sheets (Fig. 1). Thieme et al. (1981: 42) provide a sketch of the west wall showing a channel-like structure filled with reworked sediments in the uppermost part of the sequence. This channel denominated as Zone k incised into the underlying loess loam possibly during the Late Glacial (Bosinksi and Brunnacker, 1973). According to Klostermann and Thissen (1995: 45) another colluvial deposit is intercalated between the topmost humic horizon and the uppermost Bt. Instead of one Bt horizon, Schirmer and Feldmann (1992) and Schirmer (1992, 2002) identify two genetically unrelated Bt horizons (Table 1), of which the lower one is more strongly developed ("*Bt- Intensiv-Horizont*" of Cofflet, 2005: 66). In his contributions, Schirmer (2002) correlates the upper Bt horizon (Btv = Btw) with the Holocene and the lower one (Bt) with the Eemian (Last Interglacial or marine isotope stage (MIS) 5e; Table 1). This correlation was apparently supported by changes in the normal remanent magnetization within the lower Bt at ca. 70 cm below surface, claimed as representing an equivalent to the Blake event (Cofflet, 2005). However, recent dating of the Blake event as detected in speleothems revealed that it just lasted for ca. 5 kyr from ca. 115 to 110 ka (Osete et al., 2012). It is highly unlikely that this short event could be preserved near the land surface of a condensed LPS like Rheindahlen. Schirmer (2002) further postulates that Last Glacial loess is largely missing at Rheindahlen.

Below the uppermost metre of the sequence, about 2 m of yellowish-brown loess loam with finer-grained brown bands are present. This loess loam is described as *Braunlöss* (Thieme et al., 1981) or *Siltschmitzenlehm* (silt lens loam; Schirmer, 2002) and correlated with the last or penultimate glacials (Table 1; Fig. 2). A tundra gley partly superimposed by the Bt horizon is reported for the top of the *Braunlöss*, and another tundra gley is recorded in its middle part (Brunnacker, 1966; Thieme et al., 1981). Sketches of the western wall prepared by Thieme et al. (1981) and Schirmer and Feldmann (1992) show the lateral continuity of loess and palaeosol layers, which mostly run parallel. Towards the south-western corner of the brickyard, however, the thickness of the uppermost loess layer decreases and the first Bt (according to Klostermann) or first and second Bt (according to Schirmer) horizons finally merge with the one of the Erkelenz Soil.

In the northern part of the western wall, the upper loess loam has a sharp basal contact to the underlying strata. The contact delineates a channel-fill structure with dark brown, slightly more sandy sediments at the base. This erosional discontinuity, correlated with the Wetterau discordance (Schirmer, 2002), locally covers a ca. 10 cm thin layer of homogenous loess loam (Gilgau Loess). Stratigraphically below comes a ca. 50 cm thick bleached and reworked loess loam. Due to its very light colour this layer was called white band (*weisses Band, helles Band, heller Horizont*), representing an important stratigraphic marker for profile correlation within the quarry. The upper part of this layer shows a very weak grey shading and was described as Ah horizon (Paas, 1992) or Erkelenz Humus Zone (Schirmer, 2002), implying a former topsoil horizon enriched with organic matter. However, the concentration of organic carbon is very low (ca. 0.1 %) and merely enhanced in comparison to the under- and overlying strata (Schirmer, 2002: 41). The lower part of the white band shows intense redoximorphic mottling and has a slightly brown colour. It tops the reddish-brown Bt horizon of the Erkelenz Soil, about 50 to 70 cm thick. This palaeosol is correlated with the Eemian (MIS 5e) by most authors, but Schirmer (2002) suggests its correlation with MIS 7a (Table 1, Fig. 2).

The Erkelenz Soil overlays loess loam with abundant silt lenses (*Fleckenlehm* of Brunnacker, 1966; *Siltschmitzenlehm* defined as Limburg Loess according to Schirmer, 2002). The upper part of this loess loam shows local clay coatings along larger pores. In its central part, a thin layer of lighter colour and more intensive redoximorphic bleaching is mentioned and defined as Erkelenz Marker by Schirmer (2002). Other authors describe thin manganese bands (Thieme et al., 1981) or a tundra gley (Paas, 1992) at a similar stratigraphic position. Below this marker horizon, the loess is more homogenous and grades into a very slightly greyish layer defined as AhBv horizon (Paas, 1992) or Rheindahlen Humus Zone (Schirmer, 2002), the latter showing less than 0.1 % organic carbon (Schirmer, 2002: 41). The underlying Rheindahlen Soil is about 40 cm thick and has a wavy upper and diffuse lower boundary. It is correlated with either an interglacial of the Saalian complex (Paas, 1992), the Holsteinian Interglacial (MIS 9; Klostermann and Thissen, 1995), or the interglacial of MIS 7c (Schirmer, 2002). The underlying loess loam is comparatively fine-grained and shows abundant redoximorphic mottles (*Staublehm* of Brunnacker, 1966). It sandwiches the lowermost palaeosol of the sequence which was just locally preserved along the west wall. Paas (1992) ascribes a Bw horizon to this palaeosol (see also the profile description of Schirmer, 2002: 41; and Cofflet, 2005) and suggests correlation with an interstadial of the Lower Saalian, while Klostermann and Thissen (1995) identify a Bt and correlate it with the "Römerhof Interglacial" or MIS 11. Schirmer (2002, 2016) defines this palaeosol as BtBw horizon of the Wickrath Soil and suggests a correlation with MIS 7e.

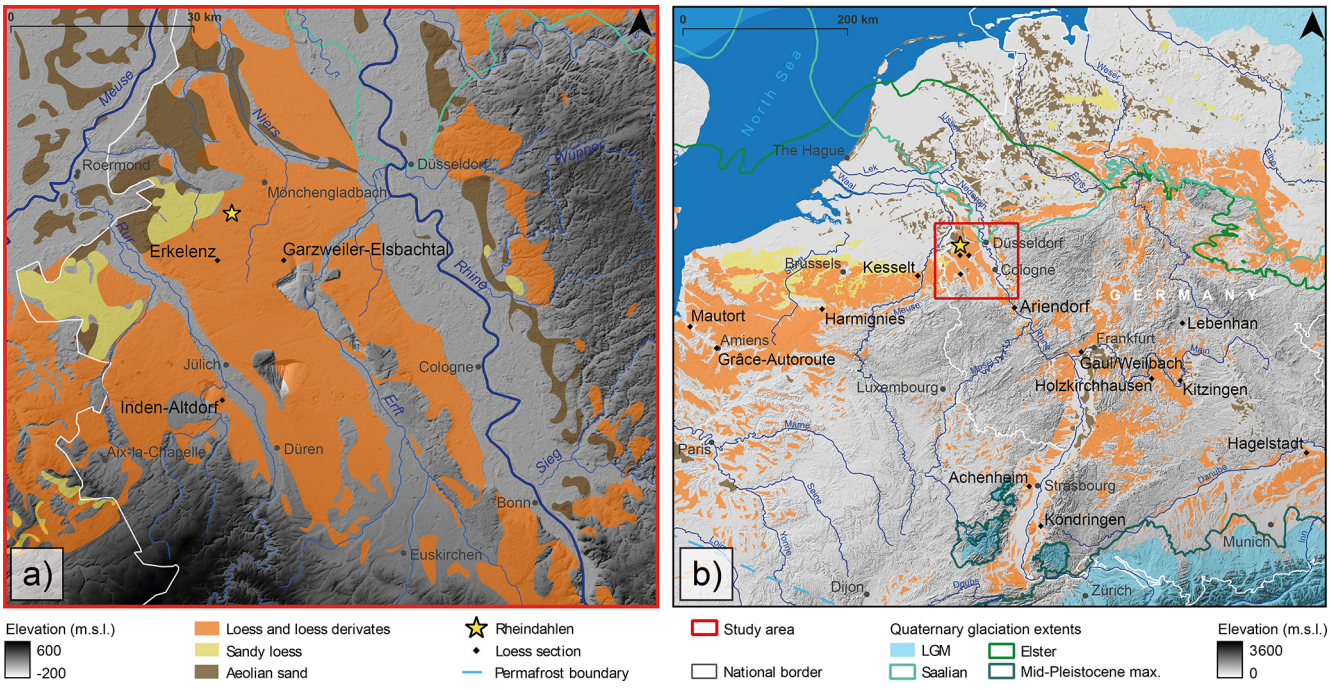

Figure 1. Loess distribution in the Lower Rhine Embayment **(a)** and in Central and Western Europe **(b)** with locations of LPSs mentioned in the text. Data sources: aeolian deposits and permafrost boundary (Lehmkuhl et al., 2021); glaciation extents (Ehlers et al., 2011); digital elevation model (EEA, 2016); rivers (Natural Earth, 2021); Rhine–Meuse tributaries (LANUV, 2021); national border (GeoBasis-DE/BKG, 2023).

At the base of the sequence, sands and gravel of the early Pleistocene younger upper terrace of the Rhine River (Hj2/3 according to Klostermann and Thissen, 1995; UT 2/3 of Boenigk and Frechen, 2006) are exposed.

2.2 Palaeolithic findings

The Palaeolithic finds from the whole of the Rheindahlen loess quarry all date to the Middle Palaeolithic, even according to Klostermann's age model. They again reflect the scientific challenge of combining technological, typological, and chronological aspects in this part of human history. In Rheindahlen, after the discovery in 1915, systematic excavations between 1964 and 2001 yielded a total of about 25 300 lithic artefacts in 10 – partly controversially discussed – find layers (Bosinski, 1966; Thieme, 1983; Thissen, 2006). There is an extreme imbalance in the quantitative proportions of finds from the individual assemblages. While layers A2, A3, B1, and B3 are relatively rich in finds, layers A1, B2, B4, B5, C1, and D1 are characterized by single finds (Thissen, 2006), some of which are very loosely scattered over the huge pit area of ca. 10 ha and thus problematic for the reconstruction of the processes on site. Apart from the stone artefacts, no organic material has been preserved in the decalcified loess.

From the long history of research on the Rheindahlen loess sequence, only the two most important aspects, which underline the importance of the site, are listed below.

The first is the discovery of an assemblage of long, narrow blades associated with small cores and correspondingly small blanks. This combination of finds did not belong to the technocomplexes established by Bosinski (1967) for western Central Europe at the end of the 1960s, which is why he extended his spectrum of complexes by one, based on the inventory of find layer B1 (Bosinski and Brunnacker, 1973): this technocomplex, which he called Rheindahlien, now includes other inventories in Germany but mainly in Belgium and northern France (Révillion and Tuffreau, 1994a; Locht et al., 2016).

In the 1980s, Hartmut Thieme's work on find layer B3 attracted attention. A total of 13 raw material nodules could be reconstructed and technologically analysed due to an extremely high refitting rate of up to 90 %. By projecting the refitting lines onto the excavation plan, the settlement dynamics of the lithic knappers became visible (Thieme, 1990).

Although the level of knowledge about the technological and typological aspects but also about the settlement dynamic processes of the two mentioned inventories, B1 and B3, is very high, there is still disagreement about their exact age position. While Richter (2016), for example, uses Schirmer's age model in his latest publications on the Palaeolithic in the Rhineland, Thissen (2006) uses Klostermann's age model in his work. This has considerable consequences for the two inventories, B1 and B3: according to Schirmer's age model they would both fall into MIS 7 and accord-

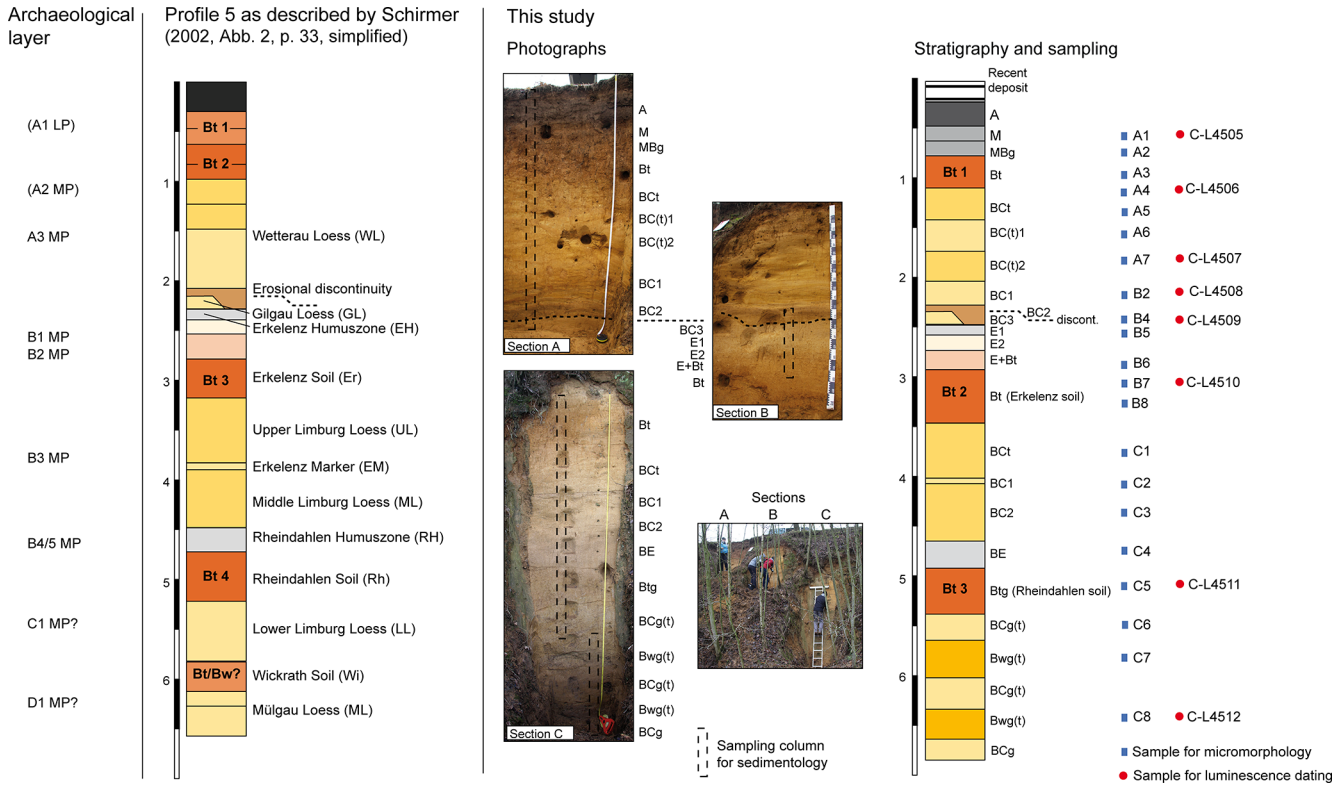

Figure 2. Stratigraphic position of Palaeolithic inventories A1 to D1 projected onto profile 5 of the Rheindahlen brickyard described by Schirmer (2002, 2016). Note that the projection of A1 and A2 is uncertain because these inventories were found in channel fills with unclear correlation to profile 5. The stratigraphic column on the right shows the sequence of profile 5 as described and sampled for this study. The dashed line is the erosional discontinuity at ca. 2.4 m depth. Key to soil horizons and sediment layers: A – former plough horizon; M – soil-derived colluvium; MBg – soil-derived colluvium with few redox concentrations; Bt – clay illuviation horizon; Bwg(t) – loess loam layer with pronounced brunification, redoximorphic mottling, and weak clay illuviation; BC – loess loam with less brunification, partly banded; BCg – loess loam with brunification and redoximorphic mottling; BC(t) – loess loam with brunification and weak clay illuviation; BE – loess loam with grey shading and weak redoximorphic mottling; E – eluvial horizon with strong redoximorphic bleaching and mottling; E+Bt – E and Bt materials in the same horizon. Horizon designations were chosen according to IUSS Working Group WRB (2022).

ing to Klostermann's age model into MIS 5a to 5d and MIS 4, respectively, resulting in an age difference of about 100 000 years. Both approaches are valid options because, with a few exceptions, there is no technological and/or typological feature in the Middle Palaeolithic that can be used unquestionably as a precise chronological marker. What can be made visible are trends in space and time.

If only those inventories of the entire Rheindahlen sequence are selected that can contribute to the discussion of the age of the loess sequence, the following five will be retained (from top to bottom):

– *Inventory A3*. The small collection of 85 stone artefacts was excavated above the white band (Thissen, 2006: 55). The finds include a quartzite hand axe of the Mousterian of Acheulian tradition (MtA) type, a small siliceous slate hand axe, and two other bifacial tools. It is mainly on the basis of the MtA hand axe that the attribution to the MtA technocomplex is discussed, which is widespread in the Late Middle Palaeolithic of early MIS 3 in Western Europe, mainly west of the Rhine River (Soressi, 2002).

– *Inventory B1*. At the level of the white band about 7300 lithic artefacts were recovered from different locations in the loess pit. In the spectrum of finds, blades, miniature cores, blanks, and Kostenki ends, which are characteristic of the Rheindahlien or Moustérien à lames, stand out. This assemblage is found in the Middle Rhine area (Conard, 1992; Conard et al., 1995, 2015), in Belgium (Otte, 1994), and in northern France (Révillion and Tuffreau, 1994b; Delagnes and Ropars, 1996; Locht et al., 2016), where the corresponding find layers date to MIS 5a to 5a (cf. Conard, 1990; Delagnes, 2000).

– *Inventory B2*. Approximately 50 cm below find layer B1 a single Micoquian hand axe was found stuck in the profile (Thieme et al., 1981: 56). Irrespective of the problem of single finds, this find would be attributed to the Micoquian (Bosinski, 2008), which was particularly

widespread in eastern Central Europe during MIS 5a to 5a/MIS 4 or MIS 4 to early MIS 3 (Bosinski, 2008; Richter, 2016; Jöris, 2003; Jöris et al., 2022). The Rhine river marks the western boundary of the main distribution area.

- *Inventory B3*. Approximately 17 500 lithic artefacts were documented in the loess at the eastern corner of the pit. In addition to the Levallois blank production, the finds include various scraper and point forms, which allow the inventory to be classified as a Mousterian–Ferrassie type (Bosinski, 2008: 126). This technocomplex is temporally and spatially unspecific but certainly belongs to the Middle Palaeolithic.

- *Inventory B5*. A total of 12 stone artefacts, including two Levallois cores, were found at the upper boundary of the Rheindahlen Bt. The artefacts certainly belong to the Middle Palaeolithic (Bosinski, 2008: 124).

The technological–typological arguments of Palaeolithic archaeology described above support Klostermann's age model, although it is also possible to fit the Palaeolithic finds from Rheindahlen into Schirmer's age model (E.-M. Ikinger, 2002). As Middle Palaeolithic archaeology can only work out tendencies, research at Rheindahlen has been stalled for a long time. Only the study of the corresponding loess formation and its dating with modern methods can help. Inventory A2, which was also relatively rich in finds and was excavated above find layer B1, consists of heavily patinated stone artefacts, some with frost cracks, distributed over large areas. According to Bosinski (2008: 213), it is uncertain whether the assemblage represents a single archaeological unit. Among the lithic artefacts there are no chronologically significant items.

3 Methods

3.1 Sampling

Three directly neighbouring sections of the western wall (sections A to C) near the original profile 5 studied by Schirmer (2002) were cleaned to reach undisturbed loess and sample the full sequence (Fig. 2 and Figs. S1, S2 in the Supplement). The major stratigraphic features described by Schirmer (2002: 33) were recognized in the new profile; however, some differences exist, as described in detail in the Results section. We used horizon designations according to IUSS Working Group WRB (2022) as pedostratigraphic codes for different sediment layers (see caption to Fig. 2).

Continuous high-resolution sampling for granulometry and spectrophotometry was accomplished by taking one sample every 5 cm for the entire LPS along vertical columns at each of the three sections. All major stratigraphic features were sampled for micromorphology by extracting undisturbed sediment blocks. Finally, eight samples were collected from the three profile sections using steel tubes for the luminescence part of the study (Figs. 2, S1, S2).

3.2 Granulometry

The samples were dried at 35 °C and sieved to the fine-earth fraction (< 2 mm), and two subsamples of each sample (0.1 and 0.3 g) were pre-treated with 0.7 mL H_2O_2 (30 %) at 70 °C for 12 h. This process was repeated until a bleaching of the material was visible (Allen and Thornley, 2004) but not longer than 3 d. To keep the particles dispersed during analysis, the samples were treated with 1.25 mL $Na_4P_2O_7 \cdot 10H_2O$ in an overhead shaker for 12 h. Grain size was determined with a Beckman Coulter LS 13320 laser diffractometer using the Mie theory (fluid RI: 1.33, sample RI: 1.55, imaginary RI: 0.1) (Schulte et al., 2016; Özer et al., 2010).

Grain size distributions (GSDs) are visualized as heatmaps (Fig. 3). This type of visualization allows us to interpret the GSD of single samples without losing vertical information of grain size parameters (Schulte et al., 2016, 2018). The heatmap visualization of the difference of the results of two different optical models (ΔGSD) can be utilized to detect neoformations of clay minerals in sediment sequences (for details see Schulte and Lehmkuhl, 2018). The grain size index (GSI) as an indicator for aeolian activity according to Rousseau et al. (2002) was calculated to complement the heatmap visualizations.

3.3 Spectrophotometry

For colorimetric analyses, air-dried samples were ground and sieved to the fine-earth fraction. Analyses were conducted according to Eckmeier and Gerlach (2012) and Vlaminck et al. (2016) using a Konica Minolta CM-5 spectrophotometer. This device uses the diffused reflected light from a standardized source (2° standard observer, illuminant C) to obtain the colour spectra of the visible light (360 to 740 nm). The results were converted to the CIELAB colour space (L*a*b*) using the SpectraMagic NX software (Konica Minolta).

3.4 Micromorphology

Block samples were extracted directly from the freshly cleaned profile wall and shipped to Thomas Beckmann (Schwülper-Lagesbüttel, Germany) for preparation of uncovered thin sections (60 mm × 80 mm, ca. 25 µm thick) using procedures described in Beckmann (1997). The thin sections were scanned using a flatbed scanner at 1200 dpi and (i) transmitted light (TL scan), (ii) transmitted light with two polarization foils placed with an orientation difference of 90° above and below the thin section (cross-polarized light, XPL, scan), and (iii) reflected light with background provided by a black isotropic foil (RL scan). The scanned images were used for investigating the thin sections at comparatively low magnification. Applying a spatial reference and multi-band image merging enabled a random-forest-based semi-supervised

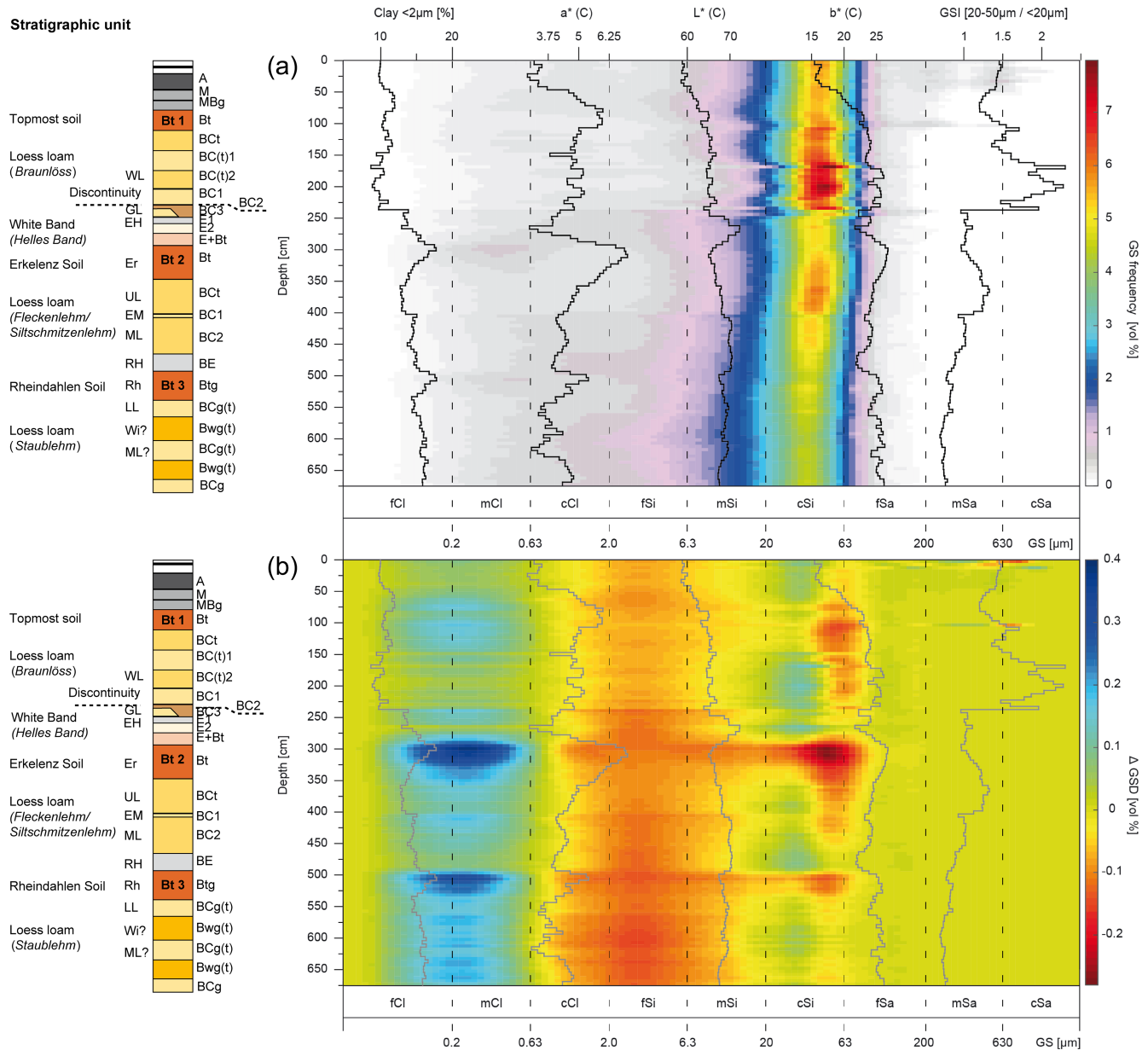

Figure 3. **(a)** Heat map visualization of the grain size distribution (GSD) frequency together with the grain size index (GSI) and colorimetric indices such as the luminance (L*) and the redness (a*). **(b)** Heat map visualization of the ΔGSD values (for details see Schulte and Lehmkuhl, 2018), also displayed with the above-mentioned proxies.

image classification of selected thin sections using the geographic information system software QGIS (Zickel et al., 2024). By classifying the thin section's content, spatial relationships and quantitative estimates – e.g. aerial percentages of clay coatings, pores, regular vs. impregnated parts of the groundmass, redoximorphic features – can be achieved. Under the microscope, the thin sections were investigated at magnifications of 12.5 ×, 25 ×, 100 ×, 200 ×, and 500 × under plane-polarized light (PPL), XPL, and oblique incident light (OIL). Circular polarized light (CPL) was used for capturing some of the micrographs as indicated in the figure captions. The description of micromorphological features follows Stoops (2021).

3.5 Luminescence dating of sediments

Polymineral fine-grain samples (4–11 µm) were prepared for luminescence dating using conventional preparation techniques (Frechen et al., 1996). Sand-sized grains were sieved to isolate the 90–125 µm fraction. Chemical treatment included HCl (10 %), H_2O_2 (10 %), and $Na_2C_2O_4$ (0.01 N) to remove carbonates, organic components, and clay. The

quartz fraction was isolated by applying density separation ($\rho = 2.62\,g\,cm^{-3}$ and $\rho = 2.68\,g\,cm^{-3}$), etched with hydrofluoric acid (37 %, 40 min), and finally washed with HCl (10 %, 1 h). All samples were measured in 2018 using an automated Risø TL/OSL DA 20 reader equipped with a calibrated ^{90}Sr beta source (dose rate $\sim 0.08\,Gy\,s^{-1}$). For quartz measurements, we used small multiple-grain aliquots (Ø 1 mm), and samples were stimulated with blue LEDs. The signals were detected through a Hoyas U340 filter (thickness: 7.5 mm). Post-infrared infrared stimulated luminescence measured at 290 °C (pIR $IRSL_{290}$; Thiel et al., 2011) and infrared stimulated luminescence measured at 50 °C (IR_{50}; Wallinga et al., 2000; Preusser, 2003) were used to measure the polymineral fine-grain samples. Stimulation was carried out with infrared LEDs (870 nm, FWHM = 40) and the signals were detected through an interference filter (410 nm). The initial 4 s of the signal minus a background of the last 20 s was used.

To design and evaluate the measurement protocols (steps of all protocols are given in Table S1), laboratory experiments included preheat plateau tests for quartz measurements, prior-IR stimulation temperature tests (Buylaert et al., 2012) for polymineral fines using a range of temperatures from 50–220 °C, and dose recovery tests. For the dose recovery test, the samples were illuminated for 24 h in a Hönle SOL2 solar simulator, and a laboratory dose in the range of the natural dose was given to the samples. Equivalent doses were calculated with an arithmetic mean. Fading tests (Auclair et al., 2003) were carried out for all samples for the IR_{50} measurement protocol. IR_{50} data were corrected for fading if g values exceeded 1 % per decade (Buylaert et al., 2012), following the approach of Kars et al. (2008) which is based on the work of Huntley (2006). For calculating the environmental dose rate, the specific activity of the radionuclides of the uranium (^{238}U) and thorium (^{232}Th) series and potassium (^{40}K) were measured using high-resolution gamma ray spectrometry (Ortec HPGe gamma ray detector). The dose rate was calculated with DRAC v.1.2 (Durcan et al., 2015), using conversion factors of Guérin et al. (2011), and a values of 0.11 ± 0.02 for pIR IRSL (Schmidt et al., 2018), 0.07 ± 0.002 for IR_{50} (Kreutzer et al., 2014), and 0.04 ± 0.01 for 90–125 µm sized quartz (Rees-Jones, 1995). As measured water contents of 4 %–11 % are likely too low to be representative of moisture over time, we used values of 18 ± 5 % which are typical for European loess (Pécsi, 1990; Klasen et al., 2015) and also comparable to those of previous studies of Frechen et al. (1992). Alpha and beta grain size attenuations followed Brennan et al. (1991) and Guérin et al. (2012). We tested the impact of potassium content on the internal beta dose rate by (i) assuming 12.5 ± 0.5 % potassium content (Huntley and Baril, 1997), (ii) assuming 10 ± 2 % (Smedley et al., 2012), (iii) assuming zero potassium content, and (iv) considering potassium concentrations obtained for dosimetry samples. As we observed no significant differences in the calculated ages and we assume the signal to be dominated by potassium, we refer to internal potassium concentrations of 10 ± 2 % (Smedley et al., 2012). The cosmic dose rate was calculated following Prescott and Hutton (1994).

4 Results

4.1 Field description

The upper part of the new profile (Fig. 2, section A) consists of an anthropogenic deposit of grey-brown silty sediments (20 cm thick) resting on a humic dark grey A horizon which represents the former plough layer (30 cm). Below the plough layer, a loosely packed grey layer (25 cm) follows. Its lower part, denominated as MBg horizon, is characterized by many iron–manganese concretions. The MBg horizon covers the first Bt horizon (35 cm) showing a reddish-brown colour and clear clay coatings in the field. We do not identify a second, genetically not related Bt at this position. The underlying yellowish-brown loess loam (130 cm thick) shows abundant brown bands of varying thickness (0.2 to 10 cm) having a mostly stretched or wavy shape (Fig. S1). Slight redoximorphic mottling is present throughout this banded loess loam. At its top, occasional clay coatings are noticed in the field (BCt, 30 cm), whereas clay coatings are rarely detected in the field in the two underlying BC(t) layers but corroborated under the microscope. The BC(t)1 layer (35 cm) has a lighter colour than the BC(t)2 layer (30 cm), which has a more homogeneous brown colour and fewer light-coloured bands. The BC1 layer (20 cm) is finely laminated and lighter coloured than the overlying BC(t)2. Contrary to Brunnacker (1966) and Schirmer (2002), a separate tundra gley in this banded loess is not clearly indicated.

On top of the erosional discontinuity at ca. 235 cm below surface, a grey-brown layer of laminated loess loam with many small iron–manganese concretions, white sediment patches, and few fine gravels occurs (BC2, 5–20 cm). This layer marks the base of the Pleistocene channel fill. The BC2 layer has a common boundary either with the remnant of the Gilgau Loess sensu Schirmer (here BC3, max 10 cm), preserved on the left side of section B only (Fig. 2), or with the upper part of the white band, here denominated as E1 (10 cm) and characterized by very weak grey shading and redoximorphic bleaching. The E1 probably represents the Ah horizon of Paas (1992) or Erkelenz Humus Zone (fAh) of Schirmer (2002). The central part (E2, 15 cm) of the white band (Fig. S1) has a very light colour and shows few and small (< 4 mm) iron–manganese concretions. Below, a layer of bleached sediment with admixtures of reddish-brown materials (E+Bt, 25 cm) represents the transition to the Bt of the Erkelenz Soil (ca. 50 cm thick). The Bt has a homogeneous reddish-brown colour, very few Fe / Mn concretions, and few clay coatings. The uppermost silt lens loam (Upper Limburg Loess) is represented by the BCt layer (50 cm) in the new profile (Fig. 2, section C, and Fig. S2). We ten-

tatively correlate a discontinuous ca. 5 cm thick sediment layer of lighter colour (BC1) with the Erkelenz Marker of Schirmer (2002). Further below, layer BC2, showing fewer silt lenses and a more homogenous yellow-brown colour than the BCt of the uppermost silt lens loam, represents the ML layer of Schirmer (2002). The Rheindahlen Humus Zone (30 cm) is indicated by a faint grey colour and less bleaching than in the E1 layer of the Erkelenz Humus Zone (see also Figs. S1 and S2). The shading is again very weak, and the horizon was thus denominated as BE. There is a wavy contact towards the underlying Bt of the Rheindahlen Soil (40 cm). The Rheindahlen Soil has a more homogenous and brown colour. Few clay coatings and few Fe / Mn concretions are present. The underlying loess (Lower Limburg Loess sensu Schirmer, 2002) is characterized by strong hydromorphic mottling (BCg(t)). Two layers within this loess have more homogeneous colours and may represent palaeosol horizons, denominated here as Bwg(t) (40 and 35 cm thick). Clay coatings were not identified in the field, though. Considering the depth of the profile, the upper of the two layers probably represents the Wickrath Soil of Schirmer (2002).

4.2 Granulometry and spectrophotometry

Generally, the Rheindahlen LPS shows typical GSDs for Central European loess sequences, as a strong mode within the coarse silt (cSi) fraction dominates the sequence (Fig. 3). There is an overall slightly coarsening trend from the base upwards. Within the Rheindahlen Soil and the underlying uppermost Lower Limburg Loess, the GSDs show relatively high contents of fine material. Clay contents increase within the Rheindahlen Soil, and high ΔGSD values in the clay fractions are indicative of the abundance of very fine particles. Typical for soil and palaeosol layers compared to loess beds, the Bt horizons also show distinct spectrophotometric characteristics, as the luminance (L*) is decreased and the redness (a*) is elevated, compared to the surrounding strata. Within the Wickrath Soil the ΔGSD values and the a* values are slightly but noticeably elevated, however, not as discrete peaks but oscillating. The grain size frequencies, L*, and GSI show no variability within the Wickrath Soil. The colour data of the Rheindahlen Humus Zone support the field description, as this pale grey layer shows increased L* values.

Although the coarse clay fraction increases within the Rheindahlen Humus Zone, the ΔGSD signal decreases, indicating depleted very fine particles. The Middle and Upper Limburg loesses surrounding the Erkelenz Marker are characterized by slightly increased ΔGSD. The Erkelenz Marker itself, however, does not show any particular signatures in grain size or colour. Nonetheless, the sediments lying above the Erkelenz Marker show some differences compared to the previously described units. The general mode of GSDs becomes coarser, and the cSi fraction increases, as contents of, for example, fine silt and coarse clay decrease. The Upper Limburg Loess between the Erkelenz Marker and the above-lying second Bt, or Erkelenz Soil, shows an elevated GSI compared to both mentioned units.

The Erkelenz Soil again shows depleted L* values and the highest a* values of the sequence, accompanied by higher clay contents, increased ΔGSD values in the fine fraction, and a sinking GSI. The above-lying white band, including the Erkelenz Humus Zone, shows the highest L* values of the sequence, with strongly decreased a* values. The Erkelenz Humus Zone appears to also be characterized by an increased ΔGSD. Above the white band, the erosional contact described above is expressed by elevated coarse and middle sand contents. Overlying this, the cSi mode is even stronger. This is accompanied by a rapid increase in the GSI, which reaches its maximum within this loess package.

The layered loess is characterized by fluctuating L* and a* values, reflecting the colour changes in the sediment. Below the first Bt, the GSI values and fine and especially middle sand contents increase, while clay values decrease. The uppermost part of the sequence is also characterized by higher sand contents, where even considerable amounts of coarse sand could be detected.

4.3 Micromorphology

A detailed micromorphological description of each thin section is provided in the Supplement (Tables S3 to S5) listing properties of the groundmass, pore space, and pedofeatures. The general trends of the microscopic observations are summarized here. The mineral composition of the loess loam is characterized by mostly silt-sized angular spherical grains of quartz and feldspar and elongated mica particles. In the Bt horizons, silt and mica are less prominent, and the proportion of the micromass (< 5 µm) is increased. Carbonate mineral grains were not found. The samples RHD A1 to A7 contain very few sand grains admixed in the silty groundmass (Fig. 4a). Only limited amounts of organic materials are identified, consisting of organic stains in the M horizon and some fresh plant root fragments in large pores in several other thin sections. Fragments of shell, bone, or lithic artefacts are not present.

A prominent basic distribution pattern of the Rheindahlen thin sections consists of bands or lenses of light-coloured silt-rich groundmass intercalated with darker-coloured bands or lenses of slightly finer groundmass (Figs. 4b, c and 5a, b). The bands have a wavy shape and often curved parallel orientation. The birefringence fabric (b-fabric) is stipple-speckled and partly grano-striated within the darker bands and lenses and weakly developed stipple-speckled in the lighter ones. Locally, a chitonic coarse–fine-related distribution, which is characterized by a network of thin and fine material covers on larger grains, is expressed in the brown bands and lenses. The banded pattern is well expressed in thin sections A5 to A7 and B4 to B6 and less strongly in A4, C6, and C7. Thin section A7 exhibits two different dimensions of banding, i.e. less than 250 µm thin and ca. 2 to 5 mm thick bands (Fig. 4c).

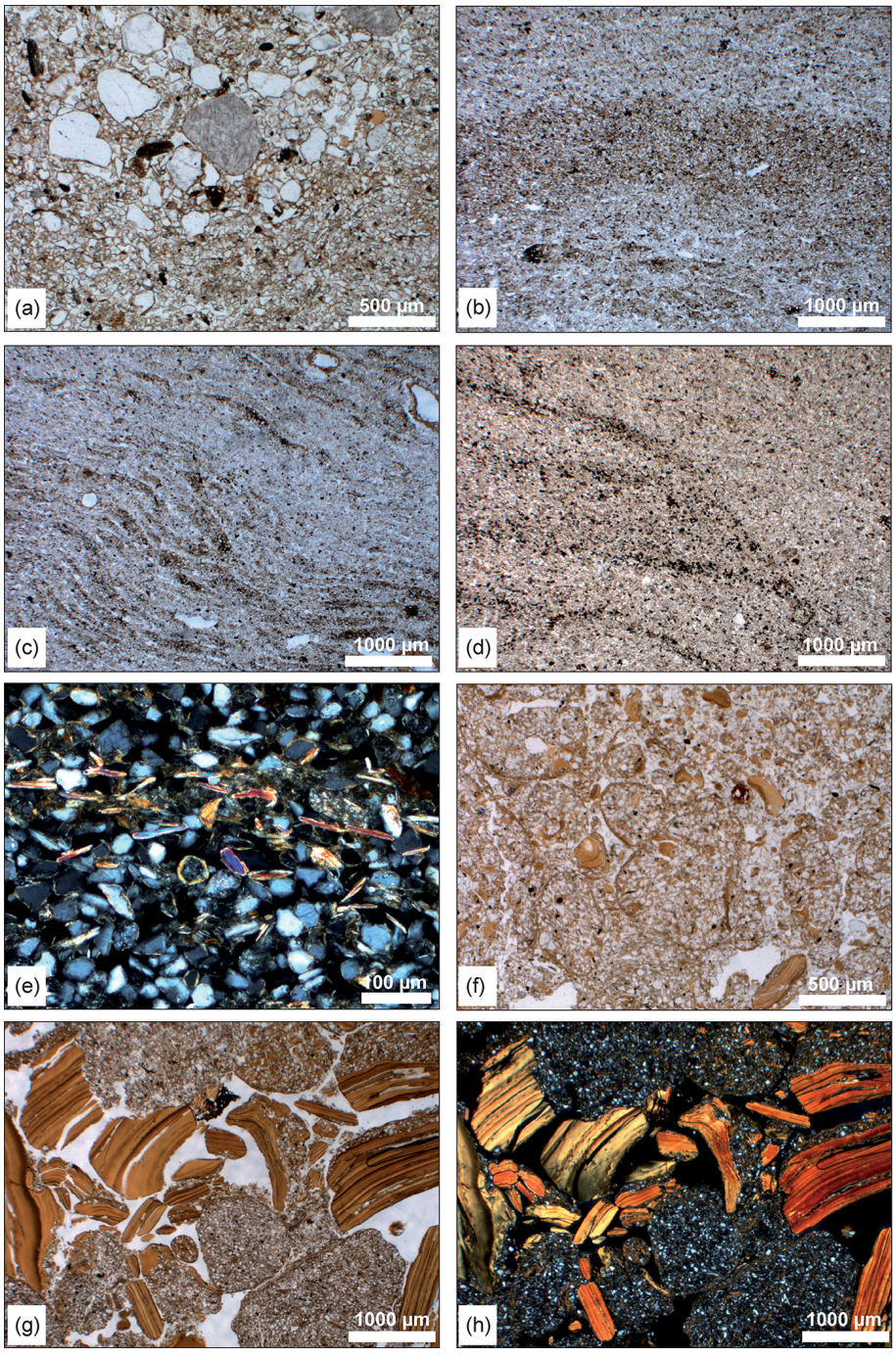

Figure 4. Selected micrographs illustrating micromorphological features. **(a)** Pocket of medium sand grains (RHD A6, PPL). **(b)** Brown band in thin section RHD A6. **(c)** Fine dark bands in thin section RHD A6. **(d)** Lamination in RHD B2. **(e)** Detail of a fine dark layer with horizontally orientated mica grains (RHD B2, CPL). **(f)** Rounded aggregates and clay papules (RHD B7). **(g)** Fragmented clay coatings and rounded aggregates (RHD B8, PPL). **(h)** Same as **(g)** but captured under circular polarized light.

Banded distribution patterns with sharp changes in the concentrations of transparent or opaque mineral grains showing cross-bedding, graded bedding, and erosional microchannels are characteristic for RHD A2 (Figs. 4e and 5c, d).

Differences in porosity are mainly related to the frequency of biogenic pores including channels, chambers, and burrows. Vughs, planes, and simple or compound packing voids formed by physical processes are less frequent. The microstructure types are spongy to subangular blocky in the

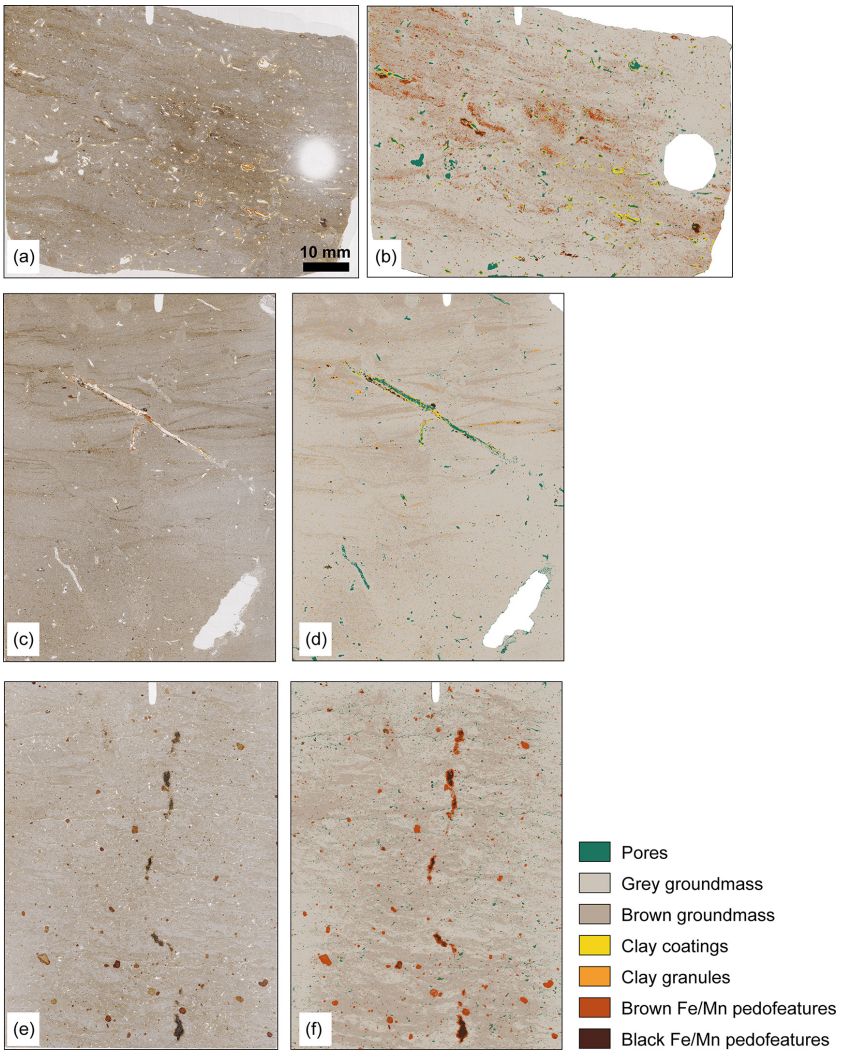

Figure 5. Thin section scans captured under transmitted light (TL, **a**, **c**, **e**) and results of a semi-supervised image classification **(b, d, f)** from three loess layers at Rheindahlen. White areas of the classification maps were excluded from the analysis. **(a, b)** Thin section RHD A7 from banded Last Glacial loess. **(c, d)** Thin section RHD B2 from the loess layer above the erosional discontinuity showing depositional features of sheet flow. Rare clay coatings in A7 (1.4 %) and B2 (0.2 % of the classified thin section area) are related to clay illuviation during the formation of the modern soil. **(e, f)** Thin section RHD B5 from the white band overlying the Erkelenz Soil. Note patchy pattern of light- and dark-coloured groundmass and lack of clay coatings.

uppermost soil horizons. The loess loam layers mostly have massive and partly platy microstructures. Rounded aggregates (Fig. 4f to h) are common in the lower part of the profile. The Bt horizons of the Erkelenz and Rheindahlen soils show higher degrees of pedality represented by subangular to angular blocky or platy microstructures (Fig. 6c, d). The micromass has a light grey or brown colour and dotted limpidity. The b-fabric is in most cases stipple-speckled, but mosaic-speckled, grano-striated, or parallel-striated types occur as well.

Pedofeatures include limpid and locally impure clay coatings found in pores or on aggregate surfaces in many thin sections but not at all or just in traces in samples RHD A1, A2, B4, and B5. Layered clay and silt coatings are found in thin sections from the Bt horizons (RHD A3, A4, B7, B8, C5) and in the *Staublehm* below the Rheindahlen Soil. Results of semi-supervised image classification of Bt horizons (Fig. 6) show that the aerial percentage of clay coatings amounts to 3.3 % in the modern Bt (RHD A4), 8.4 % in the Erkelenz Bt (RHD B7), and 2.7 % in the Rheindahlen Bt (RHD C5), reflecting different intensities of clay illuviation.

Besides these intact coatings, fragmented coatings in pores (Fig. 4g, h) are abundant in thin sections from the Erkelenz and the Rheindahlen soils and from the loess layers below (RHD B7, B8, C1, C5, C6). In addition, fragments of coatings intermixed in the silty groundmass, so-called clay

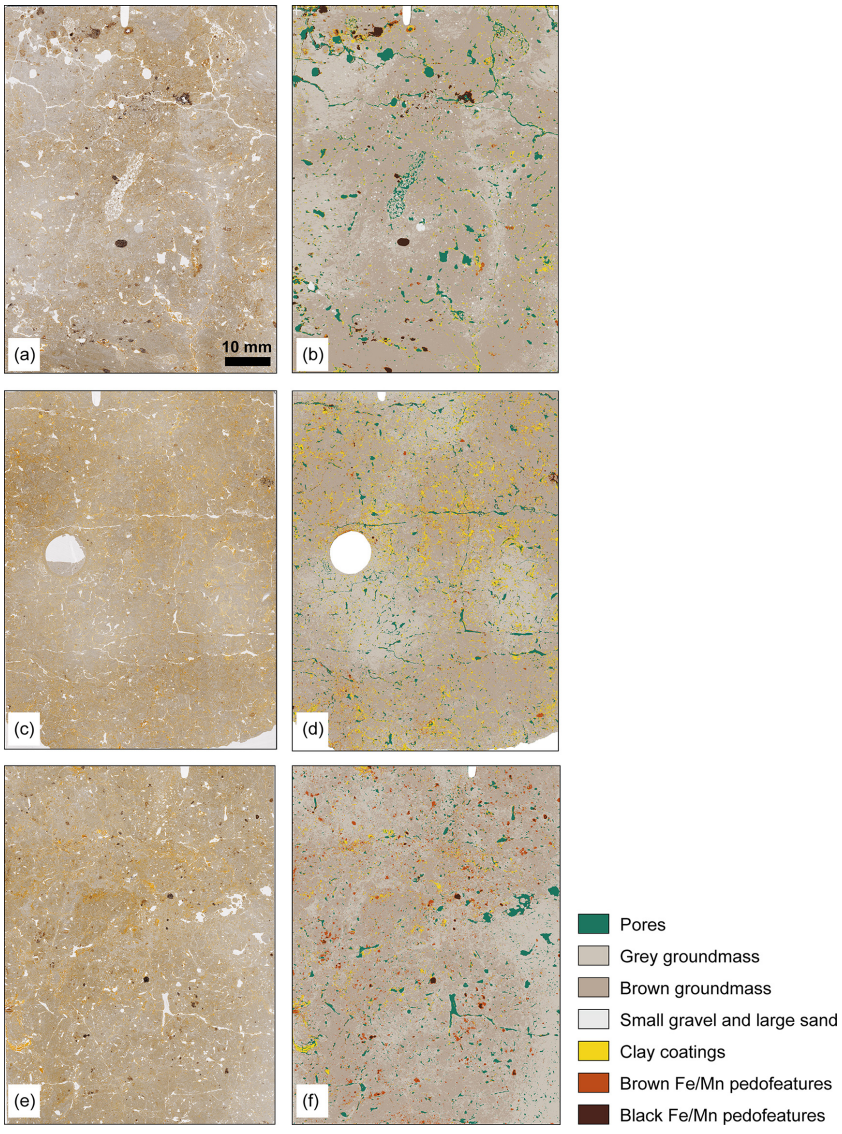

Figure 6. Thin section scans captured under ordinary transmitted light (TL, **a**, **c**, **e**) and results of supervised classification **(b, d, f)** from three different Bt horizons at Rheindahlen. White areas of the classification maps were excluded from the analysis. Note the difference in the abundance of clay coatings. **(a, b)** Thin section RHD A4 from the modern Bt horizon with clay coatings on 3.3 % of the classified area. **(c, d)** Thin section RHD B7 from the Erkelenz Soil (8.4 % clay coatings). **(e, f)** Thin section RHD C5 from the Rheindahlen Soil (2.7 % clay coatings). Small gravel and large sand grains were found in A4 only.

papules, are abundant in the middle and lower part of the profile. Silt lenses or light-coloured bands in a banded distribution pattern have comparatively low amounts of clay. They can be considered clay depletion pedofeatures assuming that the eluvial depletion of clay after the dispersion of microaggregates occurred, which is indicated by low numbers of clay domains in the groundmass. The basic distribution pattern can then be classified as clustered. However, some silt lenses consist of complete and layered silt infillings in large pores, and in that case the selective accumulation of silt is the cause for apparent lack of clay.

Redoximorphic nodules or diffuse impregnations of iron and manganese oxyhydroxides, as well as iron and manganese depletion pedofeatures, are common in most loess layers. The Fe / Mn nodules mostly have gradual outer boundaries and can be classified as orthic nodules, while few clearly disorthic ones appear in RHD A1, A2, B6, C2, and C3. They are often less than 1 mm in diameter, but some larger nodules up to 5 mm in diameter are locally present. The number of nodules is comparatively high in the modern soil (A2, A3), in the bleached zone above the Erkelenz Soil (B5, B6), and in the lowermost part of the sequence (RHD C5–C8).

Passage features are mostly vertical to diagonal channel-like compartments of the groundmass, are about 5 mm thick, and show crescent internal fabrics. These features are abundant in the uppermost 2 m of the section but less abundant, smaller, or absent below the erosional discontinuity.

4.4 Luminescence dating

Preheat plateau tests for coarse-grained quartz samples C-L4505, C-L4506, and CL-4507 revealed no dependency of the equivalent dose on temperature. Laboratory doses in the range of the natural dose were recovered within $< 5\,\%$ of unity for samples C-L4505 and C-L4506 (Fig. 7). The laboratory experiments documented the good applicability of the measurement protocol. Quartz luminescence dating reveals ages of 0.52 ± 0.11 ka (C-L4505), 13.2 ± 0.7 ka (C-L4506), and 63.9 ± 4.9 ka (C-L4507). Prior-IR stimulation temperature tests documented the good applicability of the pIR_{50} $IRSL_{290}$ protocol (Thiel et al., 2011) for samples C-L4507, C-L4508, C-L4509, and C-L4510. Laboratory doses in the range of the natural dose were recovered within $< 2\,\%$ of unity for samples C-L4507 and C-L4509 (Fig. 7). The laboratory dose of sample C-L4510 was overestimated by about 20 %, so this signal was not used for further measurements for sample C-L4510. For conventional $IRSL_{50}$ measurements (Wallinga et al., 2000; Preusser, 2003), dose recovery tests were carried out for samples C-L4507, C-L4508, C-L4509, and C-L4510, and the laboratory doses were recovered within 10 % of unity using a preheat temperature of 250 °C. The results of the laboratory experiments demonstrated the good applicability of the pIR_{50} $IRSL_{290}$ and IR_{50} measurement protocols. We have calculated polymineral fine-grain age estimates that range between ~ 110 to 146 ka for the pIR_{50} $IRSL_{290}$ signal (i.e. samples C-L4507–C-L4509) and ~ 95 to 192 ka for the fading-corrected IR_{50} signal (i.e. samples C-L4508–C-L4512; Table 2).

As the IR_{50} and the pIR_{290} signals bleach at different rates, both protocols are used for a cross-check of the measurement technique. This is especially important since the luminescence signal of quartz is saturated in samples older than C-L4507. Generally, consistent ages are a good indicator that the samples have been completely bleached prior to deposition. However, the IR_{50} signal is prone to anomalous fading, which leads to age underestimation and which has to be corrected for. Therefore, it is advantageous to measure a less fading-affected signal too, especially because fading correction is subject to a lot of assumptions. The pIR_{50} $IRSL_{290}$ signal is expected to fade less or even does not fade at all (Buylaert et al., 2012) but in turn bleaches at a lower rate. By comparing the fading-corrected IR_{50} with a pIR_{50} $IRSL_{290}$ signal, in the best case we can distinguish a partially bleached signal from a completely bleached signal. The dating results at the Rheindahlen site deliver the following findings: quartz and IR_{50} ages of sample C-L4507 are in good agreement, but the pIR_{50} $IRSL_{290}$ age is significantly older. The pIR_{50} $IRSL_{290}$ signal of sample C-L4507 most likely has not been fully bleached prior to deposition, and quartz and IR_{50} ages represent more reliable estimates for the timing of this sediment deposition instead. For samples C-L4508 and C-L4509, both IRSL ages agree within uncertainties. No pIR_{50} $IRSL_{290}$ signal was measured for sample C-L4510 because the sample did not pass the dose recovery test. While results of fading correction after Huntley (2006) indicate IR_{50} ages for samples C-L4510, C-L4511, and C-L4512 that are consistent with ages of C-L4509, they also point to an approaching field saturation of the samples. Thus, age estimates for the three lowermost luminescence samples must be used with caution and provide only minimum ages. Consequently, the lower profile section (i.e. below the erosional discontinuity where C-L4509 is located) is dated at minimum to ~ 140 kyr ago.

5 Discussion

5.1 Processes of sediment accumulation and soil formation

Granulometric and spectrometric data from the Rheindahlen LPS largely reflect the stratigraphy. Over the entire sequence, a strong mode of coarse silt typical for loess deposits prevails. A general coarsening trend from the base upwards is visible within the sequence, as the mode shifts from middle coarse silt towards the coarse silt–fine sand boundary. Overall, the grain size modes are within typical values for European LPSs (Sprafke et al., 2020). The relatively high contents of fine sand throughout the sequence point to a nearby deflation area (Frazee et al., 1970; Újvári et al., 2016; Pötter et al., 2021), which in this case is related to the alluvial plain of the Pleistocene Rhine River as a major source (Lehmkuhl et al., 2018).

The sedimentology of the Rheindahlen LPS can be subdivided in three main units, partly corroborating previous distinction in three different loess loams (Table 1). The base of the sequence, correlating with the *Staublehm* including the Rheindahlen and Wickrath soils, shows a relatively weak coarse silt mode with a low but steadily increasing GSI. Both can be the result of long-distance transport or fine particles. High ΔGSD values (Fig. 3) in the clay fractions indicate the neoformation of clay minerals and/or illuviation (Schulte and Lehmkuhl, 2018), the latter clearly indicated in thin sections. Especially the Rheindahlen Soil shows increased contents of clay and fine silt. Both grain size fractions can be affected by illuviation (Baish and Schaetzl, 2021). The next sedimentary unit starts with the Rheindahlen Humus Zone and shows increasing GSI values up to the lower boundary of the Erkelenz Bt. The strengthening of the silt mode and the sharp increase in GSI above the Erkelenz Marker show enhanced aeolian activity with augmented transport of coarse silt particles, possibly by shorter distances than before. The top of the Erkelenz Marker is interpreted as representing a discontinuity, as cor-

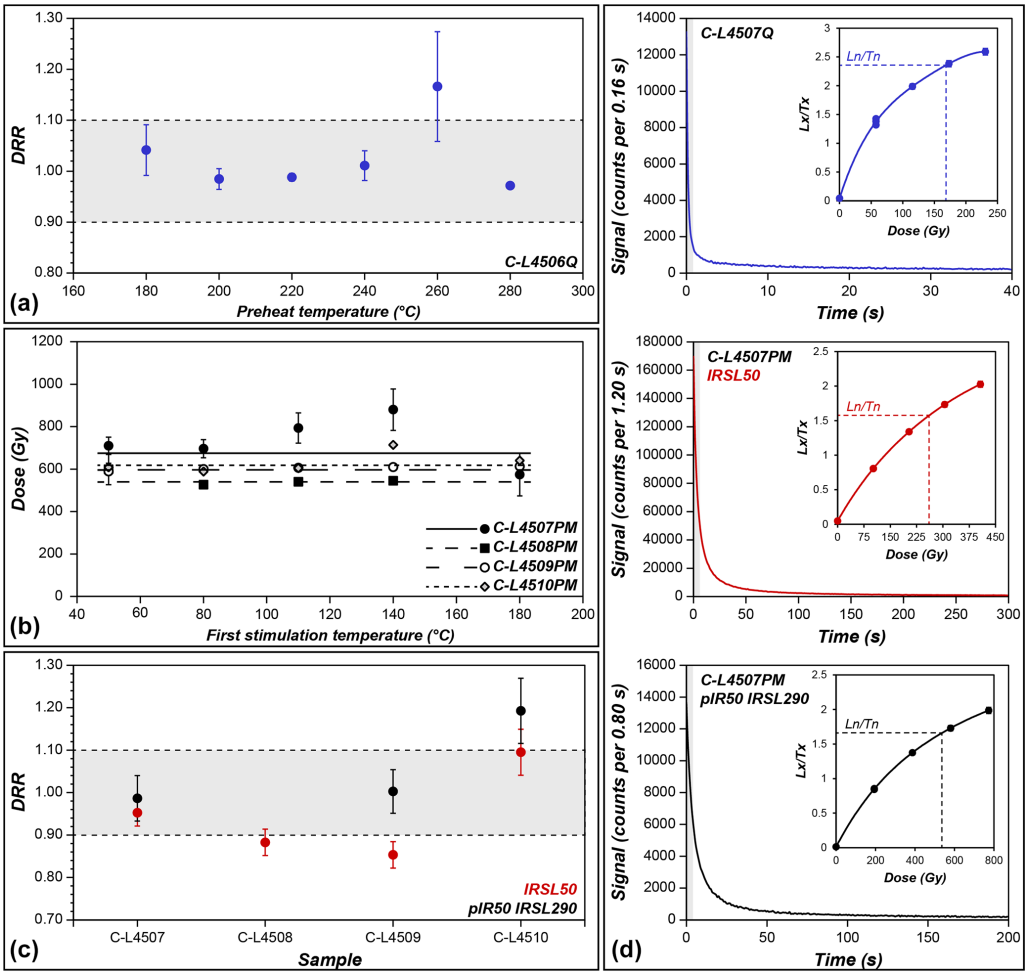

Figure 7. Results of test measurements to evaluate the applicability of the measurement protocols as well as selected luminescence properties. **(a)** Dose recovery preheat plateau test for quartz sample C-L4506. **(b)** Prior-IR stimulation temperature test for polymineral samples measured with a pIR $IRSL_{290}$ protocol. **(c)** Dose recovery ratio (DRR) for polymineral samples. Since doses from the pIR_{50} $IRSL_{290}$ signal of sample C-L4510 overestimates by about 20 %, all subsequent measurements for this sample were performed with the IR_{50} protocol. **(d)** Decay and dose response curves (as inset) for sample C-L4507. Integrated signals are highlighted.

Table 2. Summary of luminescence data obtained for all dated samples from the Rheindahlen loess–palaeosol sequence. b.s. – below surface; Q – quartz; IR – infrared stimulated luminescence; pIR IRSL – post-infrared infrared stimulated luminescence; D_e – equivalent dose; Age_{uncorr} – uncorrected ages; Age_{uncorr} – fading-corrected ages using individual g values.

Sample ID	Depth (m b.s.)	IR_{50} g value	Q D_e (Gy)	IR_{50} D_e (Gy)	pIR_{50} $IRSL_{290}$ D_e (Gy)	Q Age (ka)	IR_{50} Age_{uncorr} (ka)	IR_{50} Age_{uncorr} (ka)	pIR_{50} $IRSL_{290}$ Age_{uncorr} (ka)
C-L4505	0.55	–	1.47 ± 0.29	–	–	0.52 ± 0.11	–	–	–
C-L4506	1.10	–	35.80 ± 1.39	–	–	13.2 ± 0.7	–	–	–
C-L4507	1.80	–	181.3 ± 12.13	–	–	63.9 ± 4.9	–	–	–
C-L4507	1.80	0.68 ± 1.12	–	254.3 ± 13.58	571.6 ± 38.47	–	66.7 ± 4.3	–	133.1 ± 11.5
C-L4508	2.20	2.17 ± 0.79	–	272.7 ± 14.60	552.0 ± 27.70	–	61.7 ± 4.0	95.0 ± 7.4	109.6 ± 8.4
C-L4509	2.50	3.08 ± 1.00	–	306.3 ± 15.56	603.2 ± 31.95	–	83.6 ± 5.2	167.7 ± 12.6	145.7 ± 11.2
C-L4510	3.10	2.15 ± 1.13	–	315.5 ± 16.30	–	–	88.3 ± 5.5	138.5 ± 10.6	–
C-L4511	5.10	2.54 ± 0.99	–	373.5 ± 19.04	–	–	100.3 ± 6.2	192.0 ± 11.7	–
C-L4512	6.50	2.26 ± 1.27	–	358.4 ± 18.38	–	–	92.7 ± 5.8	154.7 ± 11.6	–

roborated by the micromorphological results. The GSI is typically decreased within the Erkelenz Soil and remains at the same level up to the erosional discontinuity mirroring the inclusion of Bt material from the Erkelenz Soil in the overlying reworked loess. The ΔGSD values of the clay fractions are elevated in the Middle Limburg Loess compared with the underlying loess of the Rheindahlen Humus Zone. Considering the rare occurrence of clay coatings, this increase is probably related to clay neoformation only. Similarly, ΔGSD values increase from the Erkelenz Marker towards the top of the Erkelenz Soil, but here clay coatings are prominent.

The loess above the erosional discontinuity represents the third unit, again showing a sharp increase in GSI to values typical for Central European Last Glacial loess deposits (Antoine et al., 2009; Zens et al., 2018). Fluctuations in grain size and a* values are strong, reflecting the banded structure of the loess.

Comparing the Rheindahlen and the Erkelenz Bt with each other, the latter shows evidence for more intense chemical weathering. Based on the maximum a* values for this unit (Fig. 3), weathering processes including rubification can be assumed, which points to warm and wet climatic conditions (Obreht et al., 2016; Barron et al., 1984). The topmost Bt, however, shows some remarkably different characteristics, especially regarding the ΔGSD, which is only slightly enhanced compared to loess layers, or even similar to initially pedogenically overprinted layers such as the white band or below the Erkelenz Marker. Nonetheless, besides the low contents of clay minerals formed in situ, other proxies for enhanced weathering or pedogenesis, especially the a* and b* values, are considerably increased and comparable or even higher to the Rheindahlen Soil (Fig. 3). Since the topmost Bt, based on its micromorphological characteristics, appears to be in situ, the differences can be explained by less intense or shorter-lasting chemical weathering. Alternatively, the topmost Bt could also represent an erosional remnant of an originally thicker horizon with more intense clay neoformation and illuviation in its lost upper part.

The micromorphological fabric provides further insights into processes of sediment deposition and post-depositional alteration. A strongly expressed banded distribution pattern with laminations, cross-bedding, graded bedding, and erosional micro rills indicate formation by low-velocity surface runoff (van der Meer and Menzies, 2011; Mücher et al., 2018). Such features are recorded in the lowermost loess layer (thin section B2) above the erosional discontinuity at 2.3 m. Only the lowermost loess loam within the channel was thus clearly reworked by surface runoff. Other loess layers show banded or clustered fabrics but lack the abovementioned characteristic features of surface runoff. These features could have been destroyed by post-depositional mixing due to solifluction or cryoturbation, processes indicated by the inclusion of sand lenses in the silty groundmass and (few) frost wedge casts within the loess layer identified in the field. However, it is more likely that the bands were not deposited by surface runoff but formed by frost activity as observed in periglacial soils (Huijzer, 1992; Kemp et al., 2001; van Vliet-Lanoë and Cox, 2018). The lack of middle and coarse sand in the bulk samples of this layer (Fig. 3) also support the periglacial overprinting, as surface runoff and other relocation processes in loess deposits are usually expressed by increased contents of these fractions (Meszner et al., 2014). Freeze–thaw is also responsible for the clustered basic distribution pattern of the *Fleckenlehm* with abundant silt lenses ("skeletspots" of Langohr and Pajares, 1983) and can be explained as follows: thawing of frozen soil or sediment causes partial or complete collapse of the soil's secondary structure and dispersion of microaggregates, processes enhanced by rainfall or snowmelt supplying low-electrolyte water. Freeze–thaw cycles thus promote separation of silt and clay (Stephan, 2000) and their downward transport with percolating water (Stephan, 2000; van Vliet-Lanoë and Cox, 2018). The fine particles are preferentially transported and deposited either as diffuse enrichments in bands or as silt cappings (silt droplets) on larger mineral grains or on aggregates. The presence of two kinds of banded fabrics was interpreted as representing several generations of ice lensing (van Vliet-Lanoë and Cox, 2018). Ice lensing and previous frost wedges are responsible for platy microstructures and layered textural infillings in oblique pores, characteristic microfeatures in the upper loess layer at Rheindahlen (see also Stephan, 1993; A. Ikinger, 2002). The deposit of the Erkelenz Marker sensu Schirmer (2002) shows several small frost wedge casts in thin section, less than 2 cm long and partly filled by silt intermixed with small clay papules. In addition, rounded aggregates and large irregular pores occur. The marker thus represents a zone of preferential frost effects in accordance with its interpretation as tundra gley (*Nassboden*; Schirmer, 2002) but was truncated as indicated by the strong increase in GSI values.

Fines mobilized under periglacial thawing conditions can also form pedofeatures such as clay coatings and infillings or thin-layered coarse clay and fine silt coatings ("mud cutans") (van Vliet-Lanoë and Cox, 2018). If such fine coatings occur together with clay coatings formed during interglacial periods, two generations of coatings (Kemp et al., 1998) may be identified. However, loess layers overlying the Bt horizons of the Rheindahlen and the Erkelenz soils are free of mud cutans indicating that the formation of coatings under periglacial conditions during corresponding loess accumulation phases did not play a role, which is also supported by generally low clay contents in these layers, as well as ΔGSD values of ~ 0.

Clay illuviation pedofeatures are very well expressed in the three Bt horizons where many clay coatings are preserved in situ in large pores. This shows that the uppermost Bt and the Erkelenz and Rheindahlen soils represent subsoils of Luvisols, developed under forest vegetation of true interglacials. Clay coatings in the banded loess below the modern soil are related to modern pedogenesis, while similarly, those found

in loess below the Erkelenz and Rheindahlen soils most probably formed during the corresponding interglacial phases. The Wickrath Soil was not clearly identified, but all three thin sections taken from below the Rheindahlen Soil show very similar types and amounts of clay coatings. In addition, most of the thin clay coatings under XPL are bright orange-brown, hence still stained by iron hydroxides, although they occur in Fe- and Mn-depleted groundmass. This shows that the strong hydromorphic mottling which characterizes the loess below the Rheindahlen Soil took place before clay illuviation. It is thus likely that most of the clay illuviation features, in particular those found in the larger pores, must be attributed to the formation of the Rheindahlen Soil. The Wickrath Soil of the lowermost loess is therefore genetically a Bw horizon, which has been transformed into a Bt horizon by overprinting during the formation of the Rheindahlen Soil, thereby corroborating the notion of Schirmer (2002). The character of a Bw horizon is underlined by the lack of a well-developed blocky microstructure and by just moderate increases in ΔGSD values and the a* values compared to the surrounding strata. Similarly, Paas (1992: 67) and Schirmer (2002: 40) did not find pronounced increases in clay contents for this layer.

Except for the first Bt and the uppermost loess, the clay coatings present in other layers are often fragmented and accompanied by high numbers of clay papules and the presence of rounded aggregates and platy microstructures. It is thus evident that the soils were strongly affected by frost during the subsequent stadials. This is not the case for the modern Bt and the clay illuviation features below reaching down to the slope wash deposit above the erosional discontinuity, as documented by limpid well-preserved clay coatings in a root channel of thin section B2. The uppermost Bt thus did not experience frost, which would have to be expected if it represented the soil of the Last Interglacial.

Sand-sized aggregates of clay (clay granules) are found in the sheetwash deposits in thin section B2 (Fig. 5c, d) and the lower part of the white band (B6). These granules show that Bt material was intermixed by surficial runoff or solifluction and underlines that both layers are zones of reworking.

Another important process of soil formation is the accumulation of organic matter, which together with abundant biopores and a crumb or spongy microstructure indicates topsoil horizons. The postulated Ah horizon and humus zones (Paas, 1992; Schirmer, 2002), at 2.6 and 4.8 m depth, do not show any of these features. From a micromorphological point of view, the grey shading identified in the field appears to be related to increased amounts of diffuse enrichment and the number of nodules of iron and manganese (hydr-)oxides. The palaeoclimatic implication and stratigraphic significance of the postulated humus zones are thus limited.

The micromorphological features, as well as the sedimentological evidence, clearly suggest that the uppermost part of the sequence consists of a colluvial layer deposited on top of the first Bt horizon. Organic stains are abundant and the porosity is very high with abundant channels and burrows, testifying to intense biological activity (Stephan, 1993). Small fragments of charcoal and the lack of clay coatings reflect the colluvial origin of this layer in comparison with the underlying first Bt (thin sections A3, A4) derived from the loess. Furthermore, the uppermost part of the sequence shows the highest sand contents, especially middle and coarse sand (Fig. 3), indicating intensive relocation by surface runoff (Antoine et al., 2003; Meszner et al., 2014; Chu et al., 2021). Banding is found only in the lowermost part of this soil, suggesting that depositional characteristics of the parental loess were lost by bioturbation. We found no evidence for the presence of two, genetically unrelated Bts as postulated by Schirmer (2002).

5.2 Chronological framing of the Rheindahlen LPS

Results of luminescence dating (Fig. 8) show that the uppermost part of the sequence compromises modern soil (C-L4505) and also includes the Bt horizon at ca. 1 m depth, which developed in sediment that was accumulated around 13.2 ± 0.7 ka (C-L4506). Micromorphology shows that this soil is in situ and not reworked, and it has not been affected by frost. Therewith, we can disprove the chronostratigraphic interpretation of Schirmer (2002), who aligned the soil to MIS 5e. According to luminescence dating, the sediment at 1.8 m depth (C-L4507) and 2.2 m depth (C-L4508) was deposited during MIS 4 (Lower Pleniglacial) or the Early Last Glacial (MIS 5a to 5d), providing clear evidence against the penultimate glacial age proposed by Schirmer (2002). In comparison to previous luminescence dating of Frechen et al. (1992) and Zöller et al. (1988), our results provide a higher temporal resolution of the uppermost part of the sequence including the Last Glacial loess and the Holocene colluvial sediments. In particular, quartz and IR_{50} ages of C-L4507 and C-L4508 are in line with a TL age of 77.2 ± 6.6 ka from loess loam sediment out of the same stratigraphic unit (Zöller et al., 1988) and are not in conflict with the TL ages provided by Frechen et al. (1992).

While insufficient signal resetting is likely the reason for overestimation of the IR_{50} age by the pIR_{50} $IRSL_{290}$ age of C-L4507, we have no explanation for the young pIR_{50} $IRSL_{290}$ age of C-L4509 compared to the IR_{50} age (Table 2). However, they agree within uncertainties and are also backed up by TL ages of 137 ± 13 ka (Zöller et al., 1988) and 163 ± 14 ka (Frechen et al., 1992). Both ages of sample C-L4509 fall into the penultimate glacial (MIS 6) but can only be interpreted with the help of the stratigraphic information. Given the facts that (i) no Eemian soil was found above sample C-L4509; (ii) the sample derives from above the white band, a zone of reworking often encountered in Western and Central European loess on top of the Eemian Bt (see below); and (iii) possible age overestimation due to imperfect bleaching in reworked sediments, the "Gilgau Loess" of the Rheindahlen sequence as postulated by Schirmer (2002) has to be interpreted as early Last Glacial loess. From an archaeolog-

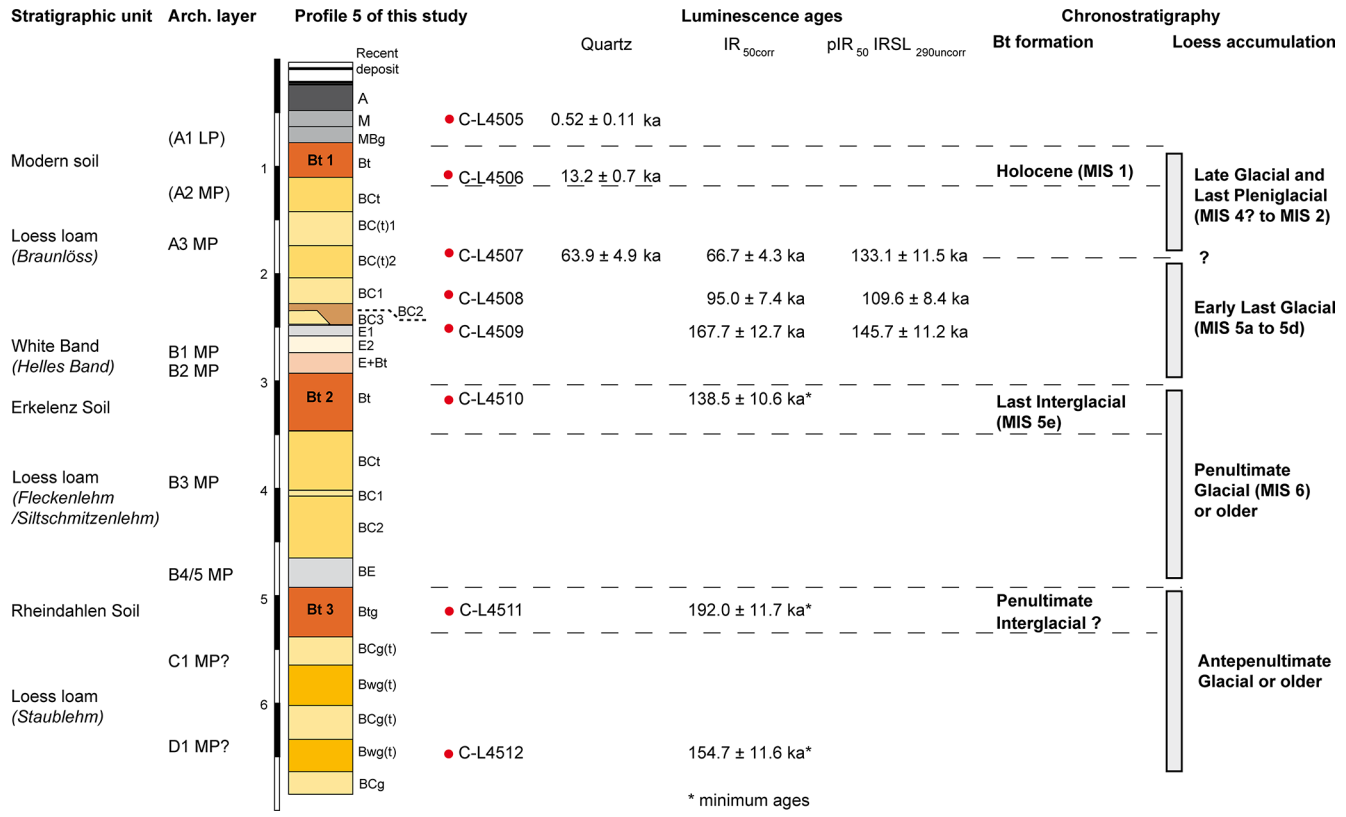

Figure 8. Correlation between main stratigraphic units, archaeological layers, and new luminescence dating results at profile 5 at Rheindahlen and a tentative chronostratigraphic assignment of the Bt horizons and intercalated loess layers.

ical point of view, it could be added that the archaeological inventories of the B1 and B2 layers are generally correlated with MIS 5a to 5d.

The luminescence age for sample C-L4510 suggests that the parental loess of the Erkelenz Soil was deposited during the penultimate interglacial (MIS 6) as would be expected for an Eemian Bt. The numerical value of the new luminescence age is very similar with the minimum age provided by Frechen et al. (1992) for the respective layer. However, all dating results from this sample and from the two lower samples provide minimum age estimates only. Thus, we can only state that the parental loess of the Erkelenz Soil and sediments below were at least deposited during MIS 6.

5.3 Synthesis of chronostratigraphic findings and implications for the age of Palaeolithic find layers

The loess loam at Rheindahlen shows strong signs of pedogenic overprint with brunification, redoximorphic mottling, and clay illuviation from overlying soil horizons. Features of reworking by surficial runoff and gelisolifluction as well as frost effects are common in loess and soil horizons below the modern Bt. Despite this complex sedimentary context, our results add new information on the chronostratigraphy of the Rheindahlen LPS, partly corroborating or rejecting previous chronostratigraphic schemes.

The top of the sequence as recorded in profile 5 consists of a former plough horizon, a layer of soil-derived colluvium, and the modern Bt horizon. The soil-derived colluvium accumulated during the Late Holocene, reflecting erosion processes under pre-industrial agricultural practices, which truncated the former topsoil horizons Ah and E of the Holocene Luvisol. The luminescence age determined for the parental loess of the modern Bt falls into the Late Glacial, probably the Younger Dryas, when a last dry and cold spell affected the Lower Rhine Embayment and may have been accompanied by the reworking of the Weichselian loess. The modern Bt does not show any features of frost and is not divided into two genetically distinct Bt horizons as assumed before (Schirmer, 2002). Abundant features of frost, testifying to periglacial climate, occur below the modern soil. In addition, our new luminescence ages place the loess layer above the erosional discontinuity into the Last Glacial, in contrast to the notion of Schirmer (2002), who suggests correlation with the penultimate glacial. One of his arguments is the lack in carbonate, noting that the upper and just locally preserved Middle Weichselian loess of the Lower Rhine Embayment contains significant amounts of carbonate. According to profile descriptions in literature, carbonate leaching on

loess of the Lower Rhine Embayment reaches 1.5 to 2.5 m depth below the modern land surface (Henze, 1998; Ikinger and Schirmer, 2002). It can therefore be assumed that leaching in the course of Holocene pedogenesis affected the entire upper loess at Rheindahlen; hence a lack of carbonate is not an indicator for the age of the layer.

Within the condensed sequence of the upper loess at Rheindahlen, the white band is a striking stratigraphic marker. Similar light-coloured reworked deposits on top of the Eemian palaeosol are described for many other LPSs of Western and Central Europe and denominated as Al horizon (e.g. Schönhals et al., 1964; Ricken, 1983), stagnic horizon (Fischer et al., 2012), or bleached horizon (Haesaerts et al., 2016). However, it should be noted that bleached horizons may also occur at other chronostratigraphic positions such as on top of each of the three soil members of the Rocourt pedocomplex (MIS 5) in Belgium (Haseaerts et al., 2016), in the global LPSs of northern France, where tonguing of leached material into the underlying Bt or Bth horizons is indicated for the Mautort I Soil of MIS 5e, as well as in the Mautort II and Mautort III soils correlated with MIS 7 (Antoine et al., 2021) or in the LPS of Lebenhan, Franconia, where three Bt horizons correlated with last and earlier interglacials are overlain by bleached zones (Rösner, 1990). However, an Early Last Glacial age of the white band at Rheindahlen is very likely because the underlying Erkelenz Bt with the Eemian (MIS 5e) is indicated by parsimonious pedostratigraphic reasoning based on counting from the top. The first fossil Bt horizon below land surface would then have the same chronostratigraphic position as the Mautort I or Grâce I Soil of the global sequence for northern France (Antoine et al., 2021), the Harmignies and Rocourt soils in Belgium (Haesaerts et al., 2016, 2019; Meijs, 2002; Meijs et al., 2013), or the Erbach Soil in the general loess stratigraphy of Germany (Schönhals et al., 1964; Semmel, 1989; Zens et al., 2018). Pedostratigraphic correlation of the first fossil Bt with the Eemian has recently been corroborated by luminescence dating at the LPS of Garzweiler–Elsbachtal and Inden–Altdorf (Fischer et al., 2012), Kitzingen and Holzkirchhausen (Rahimzadeh et al., 2021), and Köndringen (Schwahn et al., 2023).

In conclusion, loess layers in between the modern soil and the Erkelenz Soil accumulated during the Last Glacial. The correlation of the upper part of the Rheindahlen LPS with the penultimate glacial (Wetterau and Gilgau loess) is thus rejected and of the Erkelenz Soil with MIS 7a (Schirmer 2002, 2016) unlikely.

Therefore, our results strongly support placing the Middle Palaeolithic inventory of layer A3 into the Last Pleniglacial, while the inventory of layer B1, sandwiched between the Bt horizon of the Erkelenz Soil and the upper part of the white band, can probably be correlated with the Early Last Glacial. This correlation agrees with previous age assessments for the Rheindahlien (Mousterian lames from the Middle Rhine, Belgium, and northern France). The Micoquian hand axe of layer B2 would fit into this chronological frame.

The luminescence samples from the Erkelenz and the Rheindahlen Soil should be interpreted with care since the signal is near saturation, and there is no further increase in feldspar ages with depth towards the lowermost sample. In addition, the Erkelenz Marker delineates a lithostratigraphic discontinuity, which may represent a hiatus of unknown duration. Lower thickness and degree of soil development of the Rheindahlen compared to the Erkelenz Soil are noted by Paas (1962) already and are corroborated here by the lower amounts of clay coatings. Based on parsimonious reasoning using counting from the top, we tentatively place the Rheindahlen Soil into an interglacial of MIS 7. In Western and Central European loess stratigraphy, it could thus be correlated with, for instance, the Mautort II or III soils in northern France (Antoine et al., 2021), with the Hees Soil (Meijs, 2002) at Kesselt, or with the Bts of Trieux III and II (Haesaerts et al., 2019) at Harmignies in Belgium. Further correlation would be indicated with the Bt horizon beneath the Hüttenberg tephra at Ariendorf (Schmidt et al., 2014) and with the Bt horizon below the Weilbach Humus Zones (Semmel, 1968; Schmidt et al., 2011), as well as with the second pedocomplex at Achenheim (Lautridou et al., 1985; Zöller et al., 2004; Antoine et al., 2021) or the second fossil Bts at Lebenau (Rösner, 1990) or Hagelstadt (Strunk, 1990). However, the age of the Rheindahlen Soil remains tentative; hence these correlations are speculative. Human settlement testified by Palaeolithic inventories B3 and B4/5 at Rheindahlen both placed in between the Erkelenz and the Rheindahlen soils may fall into MIS 6 or older glacials.

The lowermost part of the sequence including a palaeosol (Wickrath Soil according to Schirmer) previously denominated as either Bt or Bw horizon is characterized by clay illuviation from the overlying Rheindahlen Soil. This palaeosol should be considered a polygenetic soil, not representing a "true interglacial". The weak trends in ΔGSD and a* reflect this. Therefore, the timing of the Palaeolithic inventories C1 and D1 remains open.

6 Conclusions

Revisiting the LPS at the Rheindahlen brickyard provided new insights into processes of sediment accumulation and post-depositional alteration as well as new luminescence data to re-evaluate the disputed chronostratigraphy of the sequence including its embedded stratified find horizons. Sedimentological and micromorphological analyses show differential intensities of soil development in the three Bt horizons of the modern soil, the Erkelenz Soil, and the Rheindahlen Soil, all marking interglacials. The lowermost palaeosol at Rheindahlen is polygenetic and hence cannot be correlated unequivocally with an interglacial stage but rather indicates interstadial soil formation. Frost features are common from

below the modern soil downwards providing further evidence for the Holocene age of the uppermost Bt horizons and soil-derived colluvial deposits above. Despite established measurement techniques, it was not possible to date the entire section because of luminescence signal saturation. However, the loess above the erosional discontinuity clearly accumulated during the Last Glacial, and previous correlation with the penultimate glacial must be rejected. In addition, the white band likely formed during the Early Last Glacial. Our results thus strongly support placing the Middle Palaeolithic inventories of layers A3, B1, and B2 into the Last Glacial (as expected based on typological criteria). In addition, correlation of the Erkelenz Soil with the Eemian (MIS 5e) is very likely, whereas chronological constraints and pedostratigraphy for the Rheindahlen Soil are still insufficient to propose reliable correlation. The inventories of B3 and B4/5 possibly fall into MIS 6, but a correlation with older glacials cannot be excluded. The new findings provide an improved base for stratigraphic correlation of the Rheindahlen LPS within the European loess belt and for interpreting possible diachronic changes in Neanderthal behaviour at this exceptional open-air site.

Code availability. Codes for the random-forest-based semi-supervised micromorphological soil and sediment thin section analysis are referred to in detail in Zickel et al. (2024).

Data availability. The luminescence and micromorphology data are provided in the text, Supplement, and companion paper (Zickel et al., 2024). Data records on granulometry and sediment colour can be obtained upon request from Philipp Schulte (philipp.schulte@geo.rwth-aachen.de).

Supplement. The supplement related to this article is available online at: https://doi.org/10.5194/egqsj-73-41-2024-supplement.

Author contributions. Conceptualization: MK, NK, AP. Investigation: PS, SP (granulometry, spectrometry); MK, MZ (micromorphology); KS, NK (luminescence dating). Visualization: KS, PS, SP, MK, MZ. Writing – original draft preparation: MK, AP, NK, KS, PS, SP. Writing – review and editing: MK, AP, KS, NK, PS, SP, EC. Funding acquisition: MK, EC.

Competing interests. The contact author has declared that none of the authors has any competing interests.

Disclaimer. Publisher's note: Copernicus Publications remains neutral with regard to jurisdictional claims made in the text, published maps, institutional affiliations, or any other geographical representation in this paper. While Copernicus Publications makes every effort to include appropriate place names, the final responsibility lies with the authors.

Acknowledgements. Fruitful comments and suggestions by Ludwig Zoeller, Tobias Sprafke, and an anonymous reviewer helped to substantially improve the manuscript. We are grateful for financial support for luminescence dating by the Fritz Thyssen Foundation (Cologne, Germany, grant no. 20.18.0.033AA). Sedimentological and spectrophotometric analyses were funded by the Deutsche Forschungsgemeinschaft (DFG, German Research Foundation) – project number 57444011 – CRC 806 "Our Way to Europe". We acknowledge support for the article processing charge from the DFG (German Research Foundation, 491454339).

Financial support. This research has been supported by the Fritz Thyssen Stiftung (grant no. 20.18.0.033AA) and the Deutsche Forschungsgemeinschaft (grant nos. 57444011 and 491454339).

This open-access publication
was funded by Universität zu Köln.

Review statement. This paper was edited by Tobias Sprafke and reviewed by Ludwig Zoeller and one anonymous referee.

References

Aitken, M. J.: An introduction to optical dating: the dating of Quaternary sediments by the use of photon-stimulated luminescence, Oxford University Press Inc., New York, 267 pp., ISBN 0198540922, 1998.

Allen, J. R. and Thornley, D. M.: Laser granulometry of Holocene estuarine silts: effects of hydrogen peroxide treatment, Holocene, 14, 290–295, https://doi.org/10.1191/0959683604hl681rr, 2004.

Antoine, P., Catt, J., Lautridou, J.-P., and Sommé, J.: The loess and coversands of northern France and southern England, J. Quaternary Sci., 18, 309–318, https://doi.org/10.1002/jqs.750, 2003.

Antoine, P., Rousseau, D.-D., Moine, O., Kunesch, S., Hatté, C., Lang, A., Tissoux, H., and Zöller, L.: Rapid and cyclic aeolian deposition during the Last Glacial in European loess: a high-resolution record from Nussloch, Germany, Quaternary Sci. Rev., 28, 2955–2973, https://doi.org/10.1016/j.quascirev.2009.08.001, 2009.

Antoine, P., Coutard, S., Bahain, J.-J., Locht, J.-L., Hérisson, D., and Goval, E.: The last 750 ka in loess–palaeosol sequences from northern France: environmental background and dating of the western European Palaeolithic, J. Quaternary Sci., 36, 1293–1310, https://doi.org/10.1002/jqs.3281, 2021.

Auclair, M., Lamothe, M., and Huot, S.: Measurement of anomalous fading for feldspar IRSL using SAR, Radiat. Meas., 37, 487–492, https://doi.org/10.1016/S1350-4487(03)00018-0, 2003.

Baish, C. J. and Schaetzl, R. J.: New insights into the origin and evolution of glossic features in coarse-textured soils in northern lower Michigan (USA), Soil Sci. Soc. Am. J., 85, 2115–2134, https://doi.org/10.1002/saj2.20331, 2021.

Barron, V., Rendon, J. L., Torrent, J., and Serna, C. J.: Relation of Infrared, Crystallochemical, and Morphological Properties of Al-Substituted Hematites, Clay. Clay Miner., 32, 475–479, https://doi.org/10.1346/CCMN.1984.0320605, 1984.

Beckmann, T.: Präparation bodenkundlicher Dünnschliffe für mikromorphologische Untersuchungen, Hohenheimer Bodenkundliche Hefte, 40, 89–103, 1997.

Bibus, E., Frechen, M., Kösel, M., and Rähle, W.: Das jungpleistozäne Lössprofil von Nussloch (SW-Wand) im Aufschluss der Heidelberger Zement AG, E&G Quaternary Sci. J., 56, 227–255, https://doi.org/10.3285/eg.56.4.01, 2007.

Blaauw, M., Wohlfarth, B., Christen, J. A., Ampel, L., Veres, D., Hughen, K. A., Preusser, F., and Svensson, A.: Were last glacial climate events simultaneous between Greenland and France? A quantitative comparison using non-tuned chronologies, J. Quaternay Sci., 25, 387–394, https://doi.org/10.1002/jqs.1330, 2010.

Boenigk, W. and Frechen, M.: The Pliocene and Quaternary fluvial archives of the Rhine system, Quaternary Sci. Rev., 25, 550–574, https://doi.org/10.1016/j.quascirev.2005.01.018, 2006.

Bosinski, G.: Der paläolithische Fundplatz Rheindahlen, Ziegelei Dreesen, Westwand, Bonner Jahrbücher, 166, 318–343, 1966.

Bosinski, G.: Die mittelpaläolithischen Funde im westlichen Mitteleuropa, Fundamenta A, 4, Böhlau, Köln, Graz, 205 pp., 1967.

Bosinski, G.: Urgeschichte am Rhein, Kerns-Verlag, Tübingen, ISBN 978-3-935751-09-4, 2008.

Bosinski, G. and Brunnacker, K.: Eine neue mittelpaläolithische Fundschicht in Rheindahlen, Archäol. Korresponden., 3, Heft 1, 1–6, von Zabern, Mainz, 1973.

Brennan, B. J., Lyons, R. G., and Phillips, S. W.: Attenuation of alpha particle track dose for spherical grains, International Journal of Radiation Applications and Instrumentation. Part D. Nuclear Tracks and Radiation Measurements, 18, 249–253, https://doi.org/10.1016/1359-0189(91)90119-3, 1991.

Brunnacker, K.: Das Profil "Westwand" der Ziegeleigrube Dreesen in Rheindahlen, Bonner Jahrbücher, 166, 344–356, https://doi.org/10.11588/BJB.1965.0.73844, 1966.

Buggle, B., Hambach, U., Glaser, B., Gerasimenko, N., Marković, S., Glaser, I., and Zöller, L.: Stratigraphy, and spatial and temporal paleoclimatic trends in Southeastern/Eastern European loess–paleosol sequences, Quatern. Int., 196, 86–106, https://doi.org/10.1016/j.quaint.2008.07.013, 2009.

Buylaert, J.-P., Jain, M., Murray, A. S., Thomsen, K. J., Thiel, C., and Sohbati, R.: A robust feldspar luminescence dating method for Middle and Late Pleistocene sediments, Boreas, 41, 435–451, https://doi.org/10.1111/j.1502-3885.2012.00248.x, 2012.

Chu, W., Pötter, S., Doboş, A., Albert, T., Klasen, N., Ciornei, A., Bösken, J. J., and Schulte, P.: Geoarchaeology and geochronology of the Upper Palaeolithic site of Temereşti Dealu Vinii, Banat, Romania: Site formation processes and human activity of an open-air locality, Quartär, 66, 111–134, https://doi.org/10.7485/QU66_5, 2021.

Cofflet, L.: Paläomagnetische Untersuchungen im Rheinischen Löss, Dissertation Mathematisch- Naturwissenschaftliche Fakultät, Heinrich-Heine-Univ. Düsseldorf, Düsseldorf, 152 pp., https://docserv.uni-duesseldorf.de/servlets/DocumentServlet?id=3012 (last access: 30 August 2023), 2005.

Conard, N. J.: Laminar lithic assemblages from the last interglacial complex in Northwestern Europe, J. Anthropol. Res., 46, 243–262, 1990.

Conard, N. J.: Tönchesberg and its Position in the Paleolithic Prehistory of Northern Europe, Monographien. Römisch-Germanisches Zentralmuseum, 20, Dr. Rudolf Habelt, Bonn, 176 pp., ISBN 978-3-774-92582-3, 1992.

Conard, N. J., Adler, D. S., Forrest, D. T., and Kaszas, P. J.: Preliminary archaeological results from the 1991-1993 excavations in Wallertheim, Archäol. Korresponden., 25, 13–27, 1995.

Conard, N. J., Serangeli, J., Böhner, U., Starkovich, B. M., Miller, C. E., Urban, B., and van Kolfschoten, T.: Excavations at Schöningen and paradigm shifts in human evolution, Special Issue: Excavations at Schöningen: New Insights into Middle Pleistocene Lifeways in Northern Europe, J. Hum. Evol., 89, 1–17, https://doi.org/10.1016/j.jhevol.2015.10.003, 2015.

Delagnes, A.: Blade production during the Middle Paleolithic in northwestern Europe, Acta Anthropologica Sinica, 19, 169–176, 2000.

Delagnes, A. and Ropars, A.: Paléolithique moyen en Pays de Caux (Haute-Normandie): Le Pucheuil, Etoutteville: deux gisements de plein air en milieu loessique, Documents d'Archéologie Française, 56, Maison des Sciences de l'Homme, Paris, 1996.

Durcan, J. A., King, G. E., and Duller, G. A.: DRAC: Dose Rate and Age Calculator for trapped charge dating, Quat. Geochronol., 28, 54–61, https://doi.org/10.1016/j.quageo.2015.03.012, 2015.

Eckmeier, E. and Gerlach, R.: Characterization of Archaeological Soils and Sediments Using VIS Spectroscopy, in: Journal for Ancient Studies: Proceedings of the International Conference on Landscape Archaeology, Berlin, Germany, 6–8 June 2012, edited by: ETopoi, Berlin, 285–290, https://doi.org/10.17169/REFUBIUM-21739, 2012.

EEA (European Environment Agency): European Digital Elevation Model (EU-DEM), version 1.1, Copernicus Land Monitoring Service, European Union, https://land.copernicus.eu/imagery-in-situ/eu-dem/eu-dem-v1.1?tab=download (last access: 5 September 2023), 2016.

Ehlers, J., Gibbard, P. L., and Hughes, P. D. (Eds.): Quaternary Glaciations – Extent and Chronology, Developments in Quaternary Sciences, 15, Elsevier, 1108 pp., ISBN 978-0-444-53447-7, 2011.

Fischer, P., Hilgers, A., Protze, J., Kels, H., Lehmkuhl, F., and Gerlach, R.: Formation and geochronology of Last Interglacial to Lower Weichselian loess/palaeosol sequences – case studies from the Lower Rhine Embayment, Germany, E&G Quaternary Sci. J., 61, 48–63, https://doi.org/10.3285/eg.61.1.04, 2012.

Fischer, P., Hambach, U., Klasen, N., Schulte, P., Zeeden, C., Steininger, F., Lehmkuhl, F., Gerlach, R., and Radtke, U.: Landscape instability at the end of MIS 3 in western Central Europe: evidence from a multi proxy study on a Loess-Palaeosol-Sequence from the eastern Lower Rhine Embayment, Germany, Quatern. Int., 502, 119–136, https://doi.org/10.1016/j.quaint.2017.09.008, 2019.

Fischer, P., Jöris, O., Fitzsimmons, K. E., Vinnepand, M., Prud'homme, C., Schulte, P., Hatté, C., Hambach, U., Lindauer, S., Zeeden, C., Peric, Z., Lehmkuhl, F., Wunderlich, T., Wilken, D., Schirmer, W., and Vött, A.: Millennial-scale terrestrial ecosystem responses to Upper Pleistocene climatic changes: 4D-reconstruction of the Schwalbenberg Loess-Palaeosol-Sequence (Middle Rhine Valley, Germany), Catena, 196, 104913, https://doi.org/10.1016/j.catena.2020.104913, 2021.

Frazee, C. J., Fehrenbacher, J. B., and Krumbein, W. C.: Loess Distribution from a Source, Soil Sci. Soc. Am. J., 34, 296–301, https://doi.org/10.2136/sssaj1970.03615995003400020032x, 1970.

Frechen, M., Brückner, H., and Radtke, U.: A comparison of different TL-techniques on loess samples from rheindahlen (F.R.G.), Quaternary Sci. Rev., 11, 109–113, https://doi.org/10.1016/0277-3791(92)90050-I, 1992.

Frechen, M., Schweitzer, U., and Zander, A.: Improvements in sample preparation for the fine grain technique, Ancient TL, 14, 15–17, 1996.

GeoBasis-DE/BKG: VG2500, ID: a6673ef4-6181-4448-a8a3-5e1f7f5002ef, Datenlizenz Deutschland – Zero – Version 2.0, https://www.geoportal.de/Info/a6673ef4-6181-4448-a8a3-5e1f7f5002ef (last access: 5 September 2023), 2023.

Guérin, G., Mercier, N., and Adamciec, G.: Dose-rate conversion factors: update, Ancient TL, 29, 5–8, 2011.

Guérin, G., Mercier, N., Nathan, R., Adamiec, G., and Lefrais, Y.: On the use of the infinite matrix assumption and associated concepts: A critical review, Radiat. Meas., 47, 778–785, https://doi.org/10.1016/j.radmeas.2012.04.004, 2012.

Haesaerts, P., Borziac, I., Chekha, V. P., Chirica, V., Damblon, F., Drozdov, N. I., Orlova, L. A., Pirson, S., and van der Plicht, J.: Climatic Signature and Radiocarbon Chronology of Middle and Late Pleniglacial Loess from Eurasia: Comparison with the Marine and Greenland Records, Radiocarbon, 51, 301–318, https://doi.org/10.1017/S0033822200033841, 2009.

Haesaerts, P., Damblon, F., Gerasimenko, N., Spagna, P., and Pirson, S.: The Late Pleistocene loess-palaeosol sequence of Middle Belgium, Quatern. Int., 411, 25–43, https://doi.org/10.1016/j.quaint.2016.02.012, 2016.

Haesaerts, P., Dupuis, C., Spagna, P., Damblon, F., Balescu, S., Jadin, I., Lavachery, P., Pirson, S., and Bosquet, D.: Révision du cadre chronostratigraphique des assemblages Levallois issus des nappes alluviales du Pléistocène moyen dans le bassin de la Haine (Belgique), in: Préhistoire de l'Europe du Nord-Ouest mobilités, climats et entités culturelles. XXVIIIe Congrès préhistorique de France, Amiens, France, 30 May–4 June 2016, Actes, volume 1, Session 1 – L'Europe du Nord-Ouest au Pléistocène moyen récent, edited by: Montoya C., Fagnart J.-P., and Locht J.-L., Société préhistorique française, Paris, 179–199, ISBN 978-2-913745-79-7, 2019.

Henze, N.: Kennzeichnung des Oberwürmlösses der Niederrheinischen Bucht, Kölner Forum für Geologie und Paläontologie, 1, Geolog. Inst. d. Univ, Köln, 212 pp., ISBN 978-3-93402-700-8, 1998.

Huijzer, A. S.: Micromorphological analysis of the Late Middle and Upper Pleniglacial (Weichselian) sequence of Kesselt (Belgium), in: Bodenstratigraphie im Gebiet von Maas und Niederrhein, edited by: Arbeitskreis Paläopedologie, Kiel, 22–26, 1992.

Huntley, D. J.: An explanation of the power-law decay of luminescence, J. Phys.-Condens. Mat., 18, 1359, https://doi.org/10.1088/0953-8984/18/4/020, 2006.

Huntley, D. J. and Baril, M. R.: The K content of the K-feldspars being measured in optical dating or in thermoluminescence dating, Ancient TL, 15, 11–13, https://api.semanticscholar.org/CorpusID:101762466 (last access: 30 August 2023), 1997.

Ikinger, A.: Mikropedologische Untersuchungen rheinischer Lösse und ihre Aussagen für das Profil Rheindahlen, in: Lösse und Böden in Rheindahlen, edited by: Schirmer, W., Lit, Münster, 49–60, 2002.

Ikinger, A. and Schirmer, W. (Eds.): Loess units and solcomplexes in the Niederrhein and Mass areas, Terra Nostra, 02/1, Berlin, 128 pp., 2002.

Ikinger, E.-M.: Zur formenkundlich-chronologischen Stellung der Rheindahlener Funde: Micoquien, Rheindahlien, MTA?, in: Lösse und Böden in Rheindahlen, edited by: Schirmer, W., Lit, Münster, 79–138, 2002.

IUSS Working Group WRB: World Reference Base for Soil Resources. International soil classification system for naming soils and creating legends for soil maps, 4th edn., International Union of Soil Sciences, Vienna, Austria, ISBN 979-8-9862451-1-9, 2022.

Jöris, O.: Zur chronostratigraphischen Stellung der spätmittelpaläolithischen Keilmessergruppen: Der Versuch einer kulturgeographischen Abgrenzung einer mittelpaläolithischen Formengruppe in ihrem europäischen Kontext, Bericht der Römisch-Germanischen Kommission, 84, 51–153, https://doi.org/10.11588/berrgk.2003.84.1, 2003.

Jöris, O., Neruda, P., Wiśniewski, A., and Weiss, M.: The Late and Final Middle Palaeolithic of Central Europe and Its Contributions to the Formation of the Regional Upper Palaeolithic: A Review and a Synthesis, Journal of Paleolithic Archaeology, 5, 1–55, 2022.

Kars, R. H., Wallinga, J., and Cohen, K. M.: A new approach towards anomalous fading correction for feldspar IRSL dating – tests on samples in field saturation. Radiat. Meas., 43, 786–790, https://doi.org/10.1016/j.radmeas.2008.01.021, 2008.

Kels, H.: Bau und Bilanzierung der Lössdecke am westlichen Niederrhein, Inaug.-Diss. Heinrich-Heine Univ. Düsseldorf, Düsseldorf, 206 pp., https://docserv.uni-duesseldorf.de/servlets/DocumentServlet?id=3628 (last access: 30 August 2023), 2007.

Kemp, R. A., McDaniel, P. A., and Busacca, A. J.: Genesis and relationship of macromorphology and micromorphology to contemporary hydrological conditions of a welded Argixeroll from the Palouse in Idaho, Geoderma, 83, 309–329, https://doi.org/10.1016/S0016-7061(98)00006-8, 1998.

Kemp, R. A., Derbyshire, E., and Meng, X.: A high-resolution micromorphological record of changing landscapes and climates on the western Loess Plateau of China during oxygen isotope stage 5, Palaeogeogr. Palaeocl., 170, 157–169, https://doi.org/10.1016/S0031-0182(01)00236-X, 2001.

Klasen, N., Fischer, P., Lehmkuhl, F., and Hilgers, A.: Luminescence dating of loess deposits from the Remagen-Schwalbenberg site, Western Germany, Geochronometria, 42, 67–77, https://doi.org/10.1515/geochr-2015-0008, 2015.

Klostermann, J. and Thissen, J.: Die stratigraphische Stellung des Lößprofils von Mönchengladbach-Rheindahlen (Niederrhein), E&G Quaternary Sci. J., 45, 42–58, https://doi.org/10.3285/eg.45.1.05, 1995.

Kreutzer, S., Schmidt, C., DeWitt, R., and Fuchs, M.: The a-value of polymineral fine grain samples measured with the post-IR IRSL protocol, Radiat. Meas., 69, 18–29, https://doi.org/10.1016/j.radmeas.2014.04.027, 2014.

Langohr, R. and Pajares, G.: Chronosequence of pedogenic processes in Fraglossudalfs of the Belgian loess belt, in: Soil Mi-

cromorphology, Volume 1: Techniques and Applications, edited by: Bullock, P. and Murphy, C. P., A.B. Academic Publishers, Berkhamsted, 503–510, ISBN 0907360068, 1983.

LANUV: Fließgewässertypen NRW und LAWA, ID: 234ba68c-442c-480f-8425-f2cda2b28e31, Datenlizenz Deutschland – Zero – Version 2.0, https://www.opengeodata.nrw.de/produkte/umwelt_klima/wasser/oberflaechengewaesser/fg-typen/ (last access: 5 September 2023), 2021.

Lautridou, J. P., Sommé, J., Heim, J., Puisségur, J., and Didier Rousseau, D.: La stratigraphie des loess et formations fluviatiles d'Achenheim (Alsace): nouvelles données bioclimatiques et corrélations avec les séquences pléistocènes de la France du Nord-Ouest, Bulletin de l'Association française pour l'étude du Quaternaire, 22, 125–132, 1985.

Lehmkuhl, F., Zens, J., Krauß, L., Schulte, P., and Kels, H.: Loess-paleosol sequences at the northern European loess belt in Germany: Distribution, geomorphology and stratigraphy, Quaternary Sci. Rev., 153, 11–30, https://doi.org/10.1016/j.quascirev.2016.10.008, 2016.

Lehmkuhl, F., Pötter, S., Pauligk, A., and Bösken, J.: Loess and other Quaternary sediments in Germany, J. Maps, 14, 330–340, 2018.

Lehmkuhl, F., Nett, J. J., Pötter, S., Schulte, P., Sprafke, T., Jary, Z., Antoine, P., Wacha, L., Wolf, D., Zerboni, A., Hošek, J., Marković, S. B., Obreht, I., Sümegi, P., Veres, D., Zeeden, C., Boemke, B., Schaubert, V., Viehweger, J., and Hambach, U.: Loess landscapes of Europe – Mapping, geomorphology, and zonal differentiation, Earth Sci. Rev., 215, 103496, https://doi.org/10.1016/j.earscirev.2020.103496, 2021.

Lisiecki, L. E. and Raymo, M. E.: A Pliocene-Pleistocene stack of 57 globally distributed benthic δ^{18}O records, Paleoceanography, 20, PA1003, https://doi.org/10.1029/2004PA001071, 2005.

Locht, J.-L., Hérisson, D., Goval, E., Cliquet, D., Huet, B., Coutard, S., Antoine, P., and Feray, P.: Timescales, space and culture during the Middle Palaeolithic in northwestern France, Quatern. Int., 411, 129–148, 2016.

Lomax, J., Fuchs, M., Preusser, F., and Fiebig, M.: Luminescence based loess chronostratigraphy of the Upper Palaeolithic site Krems-Wachtberg, Austria, Quatern. Int., 351, 88–97, https://doi.org/10.1016/j.quaint.2012.10.037, 2014.

Marković, S. B., Stevens, T., Mason, J., Vandenberghe, J., Yang, S., Veres, D., Újvári, G., Timar-Gabor, A., Zeeden, C., Guo, Z., Hao, Q., Obreht, I., Hambach, U., Wu, H., Gavrilov, M. B., Rolf, C., Tomić, N., and Lehmkuhl, F.: Loess correlations – Between myth and reality, Palaeogeography, Palaeoclimatology, Palaeoecology, 509, 4–23, https://doi.org/10.1016/j.palaeo.2018.04.018, 2018.

Meijs, E., van Peer, P., and de Warrimont, J.: Geomorphologic context and proposed chronostratigraphic position of Lower Palaeolithic artefacts from the Op de Schans pit near Kesselt (Belgium) to the west of Maastricht, Neth. J. Geosci., 91, 137–157, https://doi.org/10.1017/S0016774600001554, 2013.

Meijs, E. P. M.: Loess stratigraphy in Dutch and Belgian Limburg, E&G Quaternary Sci. J., 51, 115–131, https://doi.org/10.3285/eg.51.1.08, 2002.

Menning, M.: The Stratigraphic Table of Germany 2016, Z. Dtsch. Ges. Geowiss., 169, 105–128, 2018.

Meszner, S., Kreutzer, S., Fuchs, M., and Faust, D.: Identifying depositional and pedogenetic controls of Late Pleistocene loess-paleosol sequences (Saxony, Germany) by combined grain size and microscopic analyses, Z. Geo. Supp., 58, 63–90, https://doi.org/10.1127/0372-8854/2014/S-00169, 2014.

Moine, O., Rousseau, D.-D., and Antoine, P.: The impact of Dansgaard–Oeschger cycles on the loessic environment and malacofauna of Nussloch (Germany) during the Upper Weichselian, Quaternary Res., 70, 91–104, https://doi.org/10.1016/j.yqres.2008.02.010, 2008.

Moine, O., Antoine, P., Hatté, C., Landais, A., Mathieu, J., Prud'homme, C., and Rousseau, D.-D.: The impact of Last Glacial climate variability in west-European loess revealed by radiocarbon dating of fossil earthworm granules, P. Natl. Acad. Sci. USA, 114, 6209–6214, https://doi.org/10.1073/pnas.1614751114, 2017.

Mücher, H., van Steijn, H., and Kwaad, F.: Chapter 2 – Colluvial and Mass Wasting Deposits, in: Interpretation of Micromorphological Features of Soils and Regoliths (Second Edition), edited by: Stoops, G., Marcelino, V., and Mees, F., Elsevier, 21–36, https://doi.org/10.1016/B978-0-444-63522-8.00002-4, 2018.

Natural Earth: Rivers + lake centerlines, version 5.0.0, https://www.naturalearthdata.com/downloads/10m-physical-vectors/10m-rivers-lake-centerlines/ (last access: 5 September 2023), 2021.

Obreht, I., Zeeden, C., Hambach, U., Veres, D., Marković, S. B., Bösken, J., Svirčev, Z., Bačević, N., Gavrilov, M. B., and Lehmkuhl, F.: Tracing the influence of Mediterranean climate on Southeastern Europe during the past 350 000 years, Sci. Rep., 6, 36334, https://doi.org/10.1038/srep36334, 2016.

Osete, M.-L., Martín-Chivelet, J., Rossi, C., Edwards, R. L., Egli, R., Muñoz-García, M. B., Wang, X., Pavón-Carrasco, F. J., and Heller, F.: The Blake geomagnetic excursion recorded in a radiometrically dated speleothem, Earth Planet. Sci. Lett., 353–354, 173–181, https://doi.org/10.1016/j.epsl.2012.07.041, 2012.

Otte, M.: Rocourt (Liège, Belgique): Industrie laminaire ancienne, in: Les industries laminaires au Paléolithique moyen: Actes de la table ronde internationale organisée par l'ERA 37 du CRA-CNRS à, Villeneuve-d'Ascq, France, 13–14 November 1991, edited by: Révillion, S. and Tuffreau, A., CNRS éditions, Paris, 179–186, ISBN 2-271-05218-1, 1994.

Özer, M., Orhan, M., and Işik, N. S.: Effect of Particle Optical Properties on Size Distribution of Soils Obtained by Laser Diffraction, Environ. Eng. Geosci., 16, 163–173, https://doi.org/10.2113/gseegeosci.16.2.163, 2010.

Paas, W.: Rezente und fossile Böden auf niederrheinischen Terrassen und deren Deckschichten, E&G Quaternary Sci. J., 12, 165–230, https://doi.org/10.3285/eg.12.1.13, 1962.

Paas, W.: Exkursion in den nördlichen Bereich der Niederrheinischen Bucht, in: Bodenstratigraphie im Gebiet von Maas und Niederrhein, edited by: Arbeitskreis Paläopedologie, Kiel, 62–75, 1992.

Pécsi, M.: Loess is not just the accumulation of dust, Quatern. Int., 7–8, 1–21, https://doi.org/10.1016/1040-6182(90)90034-2, 1990.

Perić, Z., Lagerbäck Adolphi, E., Stevens, T., Újvári, G., Zeeden, C., Buylaert, J.-P., Marković, S. B., Hambach, U., Fischer, P., Schmidt, C., Schulte, P., Huayu, L., Shuangwen, Y., Lehmkuhl, F., Obreht, I., Veres, D., Thiel, C., Frechen, M., Jain, M., Vött, A., Zöller, L., and Gavrilov, M. B.: Quartz OSL dating of late quaternary Chinese and Serbian loess: A cross Eurasian compar-

ison of dust mass accumulation rates, Quatern. Int., 502, 30–44, https://doi.org/10.1016/j.quaint.2018.01.010, 2019.

Pötter, S., Veres, D., Baykal, Y., Nett, J. J., Schulte, P., Hambach, U., and Lehmkuhl, F.: Disentangling Sedimentary Pathways for the Pleniglacial Lower Danube Loess Based on Geochemical Signatures, Front. Earth Sci., 9, 600010, https://doi.org/10.3389/feart.2021.600010, 2021.

Prescott, J. R. and Hutton, J. T.: Cosmic ray contributions to dose rates for luminescence and ESR dating: Large depths and long-term time variations, Radiat. Meas., 23, 497–500, https://doi.org/10.1016/1350-4487(94)90086-8, 1994.

Preusser, F.: IRSL dating of K-rich feldspars using the SAR protocol: Comparison with independent age control, Ancient TL, 21, 17–23, 2003.

Prud'homme, C., Moine, O., Mathieu, J., Saulnier-Copard, S., and Antoine, P.: High-resolution quantification of earthworm calcite granules from western European loess sequences reveals stadial-interstadial climatic variability during the Last Glacial, Boreas, 48, 257–268, https://doi.org/10.1111/bor.12359, 2019.

Rahimzadeh, N., Sprafke, T., Thiel, C., Terhorst, B., and Frechen, M.: A comparison of polymineral and K-feldspar post-infrared infrared stimulated luminescence ages of loess from Franconia, southern Germany, E&G Quaternary Sci. J., 70, 53–71, https://doi.org/10.5194/egqsj-70-53-2021, 2021.

Rees-Jones, J.: Optical dating of young sediments using fine-grain quartz, Ancient TL, 13, 9–14, 1995.

Révillion, S. and Tuffreau, A. (Eds.): Les industries laminaires au Paléolithique moyen: Actes de la table ronde internationale organisée par l'ERA 37 du CRA-CNRS à, Villeneuve-d'Ascq, France, 13–14 November 1991, Dossier de documentation archéologique, 18, CNRS éditions, Paris, 193 pp., ISBN 2-271-05218-1, 1994a.

Révillion, S. and Tuffreau, A.: Valeur et signification du débitage laminaire du gisement Paléolithique moyen de Seclin (Nord), in: Les industries laminaires au Paléolithique moyen: Actes de la table ronde internationale organisée par l'ERA 37 du CRA-CNRS à, Villeneuve-d'Ascq, France, 13–14 November 1991, edited by: Révillion, S. and Tuffreau, A., CNRS éditions, Paris, 19–44, ISBN 2-271-05218-1, 1994b.

Richter, J.: Leave at the height of the party: A critical review of the Middle Paleolithic in Western Central Europe from its beginnings to its rapid decline, Quatern. Int., 411, 107–128, https://doi.org/10.1016/j.quaint.2016.01.018, 2016.

Ricken, W.: Mittel- und Jungpleistozäne Lössdecken im südwetlichen Harzvorland: Stratigraphie, Paläopedologie, fazielle Differenzierung und Konnektierung in Flussterrassen, in: Bodenerosion, Holozaene und Pleistozaene Bodenentwicklung, edited by: Bork, H.-R. and Ricken, W., Catena-Verlag Rohdenburg, Cremlingen-Destedt, 95–138, ISBN 3923381026, 1983.

Roberts, H. M.: The development and application of luminescence dating to loess deposits: a perspective on the past, present and future, Boreas, 37, 483–507, https://doi.org/10.1111/j.1502-3885.2008.00057.x, 2008.

Rösner, U.: Die Mainfränkische Lößprovinz: Sedimentologische, pedologische und morphodynamische Prozesse der Lößbildung während des Pleistozäns in Mainfranken, Erlanger Geographische Arbeiten, 51, 289 pp., ISBN 3-920405-68-4, 1990.

Rousseau, D., Antoine, P., Hatté, C., Lang, A., Zöller, L., Fontugne, M., Othman, D., Luck, J., Moine, O., Labonne, M., Bentaleb, I., and Jolly, D.: Abrupt millennial climatic changes from Nussloch (Germany) Upper Weichselian eolian records during the Last Glaciation, Quaternary Sci. Rev., 21, 1577–1582, https://doi.org/10.1016/S0277-3791(02)00034-3, 2002.

Sabelberg, U., Mavrocordat, G., Rohdenburg, H., and Schönhals, E.: Quartärgliederung und Aufbau von Warmzeit-Kaltzeit-Zyklen in Bereichen mit Dominanz periglazialer Hangsedimente, dargestellt am Quartärprofil Dreihausen/Hessen, E&G Quaternary Sci. J., 27, 93–120, https://doi.org/10.3285/eg.27.1.09, 1976.

Scheidt, S., Berg, S., Hambach, U., Klasen, N., Pötter, S., Stolz, A., Veres, D., Zeeden, C., Brill, D., Brückner, H., Kusch, S., Laag, C., Lehmkuhl, F., Melles, M., Monnens, F., Oppermann, L., Rethemeyer, J., and Nett, J.: Chronological assessment of the Balta Alba Kurgan loess-paleosol section (Romania) – a comparative study on different dating methods for a robust and precise age model, Front. Earth Sci., 8, 598448, https://doi.org/10.3389/feart.2020.598448, 2021.

Schirmer, W.: Doppelbodenkomplexe in Erkelenz und Rheindahlen, in: Bodenstratigraphie im Gebiet von Maas und Niederrhein, edited by: Arbeitskreis Paläopedologie, Kiel, 86–94, 1992.

Schirmer, W.: Kaltzeiten und Warmzeiten im Löß, in: Terrestrische Quartärgeologie, edited by: Becker-Haumann, R. and Frechen, M., Logabook, Köln, 81–100, ISBN 3-934346-03-0, 1999.

Schirmer, W. (Ed.): Lösse und Böden in Rheindahlen, GeoArchaeoRhein, 5, Lit, Münster, 138 pp., ISBN 3-8258-6008-6, 2002.

Schirmer, W.: Late Pleistocene loess of the Lower Rhine, Quatern. Int., 211, 44–61, https://doi.org/10.1016/j.quaint.2016.01.034, 2016.

Schirmer, W. and Feldmann, L.: Das Lößprofil von Rheindahlen/Niederrhein, in: Bodenstratigraphie im Gebiet von Maas und Niederrhein, edited by: Arbeitskreis Paläopedologie, Kiel, 76–85, 1992.

Schmidt, C., Bösken, J., and Kolb, T.: Is there a common alpha-efficiency in polymineral samples measured by various infrared stimulated luminescence protocols?, Geochronometria, 45, 160–172, https://doi.org/10.1515/geochr-2015-0095, 2018.

Schmidt, E. D., Semmel, A., and Frechen, M.: Luminescence dating of the loess/palaeosol sequence at the gravel quarry Gaul/Weilbach, Southern Hesse (Germany), E&G Quaternary Sci. J., 60, 9, https://doi.org/10.3285/eg.60.1.08, 2011.

Schmidt, E. D., Tsukamoto, S., Frechen, M., and Murray, A. S.: Elevated temperature IRSL dating of loess sections in the East Eifel region of Germany, Quatern. Int., 334-335, 141–154, https://doi.org/10.1016/j.quaint.2014.03.006, 2014.

Schönhals, E., Rohdenburg, H., and Semmel, A.: Ergebnisse neuerer Untersuchungen zur Würmlöß-Gliederung in Hessen, E&G Quaternary Sci. J., 15, 199–206, https://doi.org/10.3285/eg.15.1.15, 1964.

Schulte, P. and Lehmkuhl, F.: The difference of two laser diffraction patterns as an indicator for post-depositional grain size reduction in loess-paleosol sequences, Palaeogeogr. Palaeocl., 509, 126–136, https://doi.org/10.1016/j.palaeo.2017.02.022, 2018.

Schulte, P., Lehmkuhl, F., Steininger, F., Loibl, D., Lockot, G., Protze, J., Fischer, P., and Stauch, G.: Influence of HCl pretreatment and organo-mineral complexes on laser diffraction measurement of loess–paleosol-sequences, Catena, 137, 392–405, https://doi.org/10.1016/j.catena.2015.10.015, 2016.

Schulte, P., Sprafke, T., Rodrigues, L., and Fitzsimmons, K. E.: Are fixed grain size ratios useful proxies for loess sedimentation dynamics? Experiences from Remizovka, Kazakhstan, Aeolian Res., 31, 131–140, https://doi.org/10.1016/j.aeolia.2017.09.002, 2018.

Schwahn, L., Schulze, T., Fülling, A., Zeeden, C., Preusser, F., and Sprafke, T.: Multi-method study of the Middle Pleistocene loess–palaeosol sequence of Köndringen, SW Germany, E&G Quaternary Sci. J., 72, 1–21, https://doi.org/10.5194/egqsj-72-1-2023, 2023.

Semmel, A.: Studien über den Verlauf jungpleistozäner Formung in Hessen, Frankfurter Geogr. Hefte, 45, 133 pp., 1968.

Semmel, A.: The importance of loess in the interpretation of geomorphological processes and for dating in the federal republic of Germany, in: Landforms and landform evolution in West Germany: Published in connection with the Second International Conference on Geomorphology, Frankfurt a.M., 3–9 September 1989, edited by: Ahnert, F., Catena-Verl., Cremlingen-Destedt, 179–188, ISBN 3-923381-18-2, 1989.

Smedley, R. K., Duller, G. A. T., Pearce, N. J. G., and Roberts, H. M.: Determining the K-content of single-grains of feldspar for luminescence dating, Radiat. Meas., 47, 790–796, https://doi.org/10.1016/j.radmeas.2012.01.014, 2012.

Soressi, M.: Le Moustérien de tradition acheuléenne du sud-ouest de la France: Discussion sur la signification du faciès à partir de l'étude comparée de quatre sites Pech-de-l'Azé I, Le Moustier, La Rochette et la Grotte XVI, Ecole doctorale des Sciences du vivant – Géoscience, Sciences de l'environnement, Université Bordeaux I, Bordeaux, 2002.

Sprafke, T., Schulte, P., Meyer-Heintze, S., Händel, M., Einwögerer, T., Simon, U., Peticzka, R., Schäfer, C., Lehmkuhl, F., and Terhorst, B.: Paleoenvironments from robust loess stratigraphy using high-resolution color and grain-size data of the last glacial Krems-Wachtberg record (NE Austria), Quaternay Sci. Rev., 248, 106602, https://doi.org/10.1016/j.quascirev.2020.106602, 2020.

Stephan, S.: Zur mikromorphologischen Unterscheidung allochthoner und autochthoner Prozesse in den Lößderivaten und fossilen Böden von Rheindahlen – Niederrhein, Mitt. Dtsch. Bodenkundl. Ges., 72, 1065–1068, 1993.

Stephan, S.: Bt-Horizonte als Interglazial-Zeiger in den humiden Mittelbreiten: Bildung, Mikromorphologie, Kriterien, E&G Quaternary Sci. J., 50, 95–106, https://doi.org/10.3285/eg.50.1.07, 2000.

Stoops, G.: Guidelines for analysis and description of regolith thin sections, Second edition, Wiley-ACSESS, Hoboken, NJ, 240 pp., ISBN 978-0-89118-975-6, 2021.

Strunk, H.: Das Quartärprofil von Hagelstadt im Bayerischen Tertiärhügelland, E&G Quaternary Sci. J., 40, 85–96, https://doi.org/10.3285/eg.40.1.06, 1990.

Tecsa, V., Gerasimenko, N., Veres, D., Hambach, U., Lehmkuhl, F., Schulte, P., and Timar-Gabor, A.: Revisiting the chronostratigraphy of Late Pleistocene loess-paleosol sequences in southwestern Ukraine: OSL dating of Kurortne section, Quatern. Int., 542, 65–79, https://doi.org/10.1016/j.quaint.2020.03.001, 2020.

Thiel, C., Buylaert, J.-P., Murray, A., Terhorst, B., Hofer, I., Tsukamoto, S., and Frechen, M.: Luminescence dating of the Stratzing loess profile (Austria) – Testing the potential of an elevated temperature post-IR IRSL protocol, Quatern. Int., 234, 23–31, https://doi.org/10.1016/j.quaint.2010.05.018, 2011.

Thieme, H.: Der paläolithische Fundplatz Rheindahlen, Dissertation, Institut für Ur- und Frühgeschichte, Universität zu Köln, Köln, 1983.

Thieme, H.: Wohnplatzstrukturen und Fundplatzanalysen durch das Zusammenpassen von Steinartefakten: Ergebnisse vom mittelpaläolithischen Fundplatz Rheindahlen B1 (Westwand-Komplex), in: The Big Puzzle, edited by: Cziesla, E., Eickhoff, S., Arts, N., and Winter, D., Holos, Bonn, 544–568, ISBN 3-926216-94-8, 1990.

Thieme, H., Brunnacker, K., and Juvigné, E.: Petrographische und urgeschichtliche Untersuchungen im Lößprofil von Rheindahlen/Niederrheinische Bucht, Quartär, 31/32, 41–67, 1981.

Thissen, J. P.: Die paläolithischen Freilandstationen von Rheindahlen im Löss zwischen Maas und Niederrhein, Rheinische Ausgrabungen, 59, Philipp von Zabern, Mainz, ISBN 3805336721, 2006.

Timar-Gabor, A., Vandenberghe, D., Vasiliniuc, S., Panaoitu, C. E., Panaiotu, C. G., Dimofte, D., and Cosma, C.: Optical dating of Romanian loess: A comparison between silt-sized and sand-sized quartz, Quatern. Int., 240, 62–70, https://doi.org/10.1016/j.quaint.2010.10.007, 2011.

Újvári, G., Kok, J. F., Varga, G., and Kovács, J.: The physics of wind-blown loess: Implications for grain size proxy interpretations in Quaternary paleoclimate studies, Earth Sci. Rev., 154, 247–278, https://doi.org/10.1016/j.earscirev.2016.01.006, 2016.

Újvári, G., Stevens, T., Molnár, M., Demény, A., Lambert, F., Varga, G., Jull, A. J. T., Páll-Gergely, B., Buylaert, J.-P., and Kovács, J.: Coupled European and Greenland last glacial dust activity driven by North Atlantic climate, P. Natl. Acad. Sci. USA, 114, E10632-E10638, https://doi.org/10.1073/pnas.1712651114, 2017.

van der Meer, J. J. M. and Menzies, J.: The micromorphology of unconsolidated sediments, Sediment. Geol., 238, 213–232, https://doi.org/10.1016/j.sedgeo.2011.04.013, 2011.

van Vliet-Lanoë, B. and Cox, C. A.: Chapter 20 – Frost Action, in: Interpretation of Micromorphological Features of Soils and Regoliths, 2nd edn., edited by: Stoops, G., Marcelino, V., and Mees, F., Elsevier, 575–603, https://doi.org/10.1016/B978-0-444-63522-8.00020-6, 2018.

Vinnepand, M., Fischer, P., Jöris, O., Hambach, U., Zeeden, C., Schulte, P., Fitzsimmons, K. E., Prud'homme, C., Perić, Z., Schirmer, W., Lehmkuhl, F., Fiedler, S., and Vött, A.: Decoding geochemical signals of the Schwalbenberg Loess-Palaeosol-Sequences – A key to Upper Pleistocene ecosystem responses to climate changes in western Central Europe, Catena, 212, 106076, https://doi.org/10.1016/j.catena.2022.106076, 2022.

Vlaminck, S., Kehl, M., Lauer, T., Shahriari, A., Sharifi, J., Eckmeier, E., Lehndorff, E., Khormali, F., and Frechen, M.: Loess-soil sequence at Toshan (Northern Iran): Insights into late Pleistocene climate change, Quatern. Int., 399, 122–135, https://doi.org/10.1016/j.quaint.2015.04.028, 2016.

Wallinga, J., Murray, A., and Wintle, A.: The single-aliquot regenerative-dose (SAR) protocol applied to coarse-grain feldspar, Radiat. Meas., 32, 529–533, https://doi.org/10.1016/S1350-4487(00)00091-3, 2000.

Zens, J., Schulte, P., Klasen, N., Krauß, L., Pirson, S., Burow, C., Brill, D., Eckmeier, E., Kels, H., Zeeden, C., Spagna, P., and Lehmkuhl, F.: OSL chronologies of pa-

leoenvironmental dynamics recorded by loess-paleosol sequences from Europe: Case studies from the Rhine-Meuse area and the Neckar Basin, Palaeogeogr. Palaeocl., 509, 105–125, https://doi.org/10.1016/j.palaeo.2017.07.019, 2018.

Zickel, M., Gröbner, M., Röpke, A., and Kehl, M.: MiGIS: micromorphological soil and sediment thin section analysis using an open-source GIS and machine learning approach, E&G Quaternary Sci. J., 73, 69–93, https://doi.org/10.5194/egqsj-73-69-2024, 2024.

Zöller, L.: Geomorphologische und geologische Interpretation von Thermolumineszenz-Daten, Bayreuther Geowissenschaftliche Arbeiten, 14, 103–112, 1989.

Zöller, L. and Semmel, A.: 175 years of loess research in Germany – long records and "unconformities", Earth-Sci. Rev., 54, 19–28, https://doi.org/10.1016/S0012-8252(01)00039-3, 2001.

Zöller, L., Stremme, H., and Wagner, G. A.: Thermolumineszenzdatierung an Löß-Paläoboden-Sequenzen von Nieder-, Mittel- und Oberrhein/Bundesrepublik Deutschland, Chemical Geology: Isotope Geoscience section, 73, 39–62, https://doi.org/10.1016/0168-9622(88)90020-6, 1988.

Zöller, L., Rousseau, D.-D., Jäger, K.-D., and Kukla, G.: Last interglacial, Lower and Middle Weichselian – a comparative study from the Upper Rhine and Thuringian loess areas, Z. Geomorphol., 48, 1–24, https://doi.org/10.1127/zfg/48/2004/1, 2004.